Aus dem Fachbereich Medizin
der Johann Wolfgang Goethe-Universität
Frankfurt am Main

betreut am
Zentrum für Neurologie und Neurochirurgie
Klinik für Neurologie
Direktor: Prof. Dr. Helmuth Steinmetz

Sphingolipidmetabolismus in der akuten Phase der zerebralen Ischämie

Dissertation
zur Erlangung des Doktorgrades der Medizin
des Fachbereichs Medizin
der Johann Wolfgang Goethe-Universität
Frankfurt am Main

vorgelegt von
Alexandra Lucaciu

Aus Klausenburg, Rumänien

Frankfurt am Main, 2021

Dekan:	Prof. Dr. Stefan Zeuzem
Referent:	PD Dr. Robert Brunkhorst
Korreferent:	Prof. Dr. Karlheinz Plate
Tag der mündlichen Prüfung:	12.05.2022

Meiner Familie

Inhaltsverzeichnis

1. Zusammenfassung

Beim ischämischen Schlaganfall finden weitreichende systemische immunmodulatorische Anpassungsvorgänge statt. Da Sphingosin-1-Phosphat (S1P)-Signalwege für die Immunzellrekrutierung von hoher Relevanz sind, war angesichts der bekannten immunologischen Veränderungen nach zerebraler Ischämie das Ziel dieser Dissertation die genauen Veränderungen dieses Signalweges zu charakterisieren.

Für diese Charakterisierung wurde ein transientes Fadenokklusionsmodell der A. cerebri media an der Maus verwendet. Die Sphingolipidkonzentrationen wurden drei oder 24 Stunden nach Okklusion in der Milz, im Plasma sowie im Hirngewebe gemessen. Parallel hierzu wurde die Immunzellrekrutierung in die von der Ischämie betroffenen Hemisphäre analysiert.

Zunächst konnte diese Dissertation zeigen, dass in der Akutphase des Schlaganfalls ein S1P-Konzentrationsgradient vorherrscht. Die Milz zeigt hier die niedrigsten Konzentrationen, gefolgt von Plasma und Gehirn. Darüber hinaus besteht auch in der betroffenen Hemisphäre ein S1P-Gradient mit hohen Konzentrationen im Infarktkern, jedoch verminderten Konzentrationen im Periinfarktkortex (PIC).

Zweitens führt eine fokale zerebrale Ischämie zu einer Infiltration von T- und B-Lymphozyten in die ischämische Hemisphäre. Im Gegensatz hierzu kommt es zu einer Schlaganfall-induzierten Lymphopenie im Blut. Hierzu passend konnte ich eine signifikante Abnahme des Gewichts und der B- und T-Lymphozyten der Milz 24 Stunden nach Ischämie nachweisen. Weitere von Immunzellen produzierte Zytokine (IL-6) sowie deren Transkriptionsfaktoren (SPI1, STAT3, FoxP3) zeigten in der Akutphase nach Ischämie ebenfalls eine deutliche Reduktion und wiesen auf die Rekrutierung peripherer Immunzellen (pIZ) aus dem sekundären lymphatischen Organ hin. Folgerichtig waren Leukozyten im Plasma sowohl drei als auch 24 Stunden nach Ischämie signifikant vermehrt, welche insbesondere neutrophilen Granulozyten entsprachen.

Basierend auf der nachgewiesenen Reduktion von T-Helferzellen sowie regulatorischer T-Zellen sowohl in der Milz als auch in der Zirkulation, wurde drittens die Hypothese einer zerebralen Rekrutierung dieser T-Zellpopulationen gemäß

dem vorliegenden S1P-Gradienten untersucht. Dabei gelang die Darstellung einer signifikanten Infiltration von $CD45^+$-Zellen in beide Hemisphären, welche insbesondere von T-Helferzellen geprägt war.

Viertens nimmt die S1P-Rezeptor ($S1P_R$)-Expression auf Leukozyten eine bedeutende Stellung in der pIZ-Rekrutierung ein. In diesem Sinne konnte ich zeigen, dass nach zerebraler Ischämie $S1P_1$ signifikant in der Milz vermindert exprimiert wurde. Dieses Ergebnis deutete auf einen Austritt $S1P_1^+$ Immunzellen aus der Milz dem etablierten S1P-Gradienten folgend hin. In der ischämischen Hemisphäre hingegen ließ sich ebenfalls eine Herunterregulation der exprimierten mRNA für $S1P_1$ nachweisen, wohingegen $S1P_2$ und $S1P_3$ vermehrt transkribiert wurden. Dieses Ergebnis könnte Folge der mikroglialen Aktivierung sein, die bekanntermaßen mit einer Hochregulation von $S1P_2$ und $S1P_3$ einhergeht.

Abschließend habe ich die Rolle von weiteren Sphingolipiden, u.a. von Ceramiden, untersucht, die einen signifikanten Anstieg in der Milz 24 Stunden nach Ischämie zeigten. Im Gegensatz dazu konnte ich im Gehirn keine Unterschiede der untersuchten Ceramidspezies abgrenzen, sodass in dem hier verwendeten Modell eine Beteiligung an lokalen pathophysiologischen Vorgängen eher unwahrscheinlich erscheint.

Zusammenfassend beschreiben die in dieser Dissertation dargestellten Ergebnisse lokale und systemische Veränderungen des S1P-Signalwegs nach zerebraler Ischämie. Konkordante Veränderungen des Immunsystems deuten auf eine relevante Rolle veränderter S1P-Konzentrationen hin. Weitergehende, funktionelle Untersuchungen der hier beobachteten Ergebnisse müssen die potentielle therapeutische Relevanz für Patienten mit zerebraler Ischämie aufklären.

2. Summary

Ischemic stroke exerts extensive systemic adaptive immunomodulatory responses. S1P-signaling pathways play an important role in immune cell recruitment and given the known immune response alterations following stroke, the aim of this dissertation was to provide a detailed characterization of the S1P signaling pathway.

For this characterization, a transient filament occlusion model of the mouse middle cerebral artery was implemented. Sphingolipid concentrations were measured three or 24 hours after occlusion in spleen, plasma and brain tissue. In parallel, immune cell recruitment was analysed in the hemisphere affected by ischemia.

First of all, this thesis could demonstrate a steep S1P gradient in the acute phase of stroke. The spleen showed the lowest S1P concentrations, followed by plasma and brain. In addition, there was a significant S1P increase in the ischemic hemisphere, whereas the peri-infarct cortex (PIC) showed decreased S1P levels.

Secondly, focal cerebral ischemia induces an inflammatory cascade which is denoted by an early infiltration of T and B lymphocytes. This phenomenon was reflected systemically leading to a stroke-induced lymphopenia in the circulation. In accordance with this result, I could demonstrate a significant weight reduction of the spleen and a decrease of B and T lymphocytes in the spleen 24 h after ischemia. Other cytokines produced by immune cells (IL-6) as well as their transcription factors (SPI1, STAT3, FoxP3) showed a significant reduction in the acute phase after ischemia and underlined the recruitment of peripheral immune cells (pIZ) from the secondary lymphoid organ. Consequently, especially neutrophil granulocytes in plasma were increased three hours and 24 hours after ischemia.

Thirdly, based on the reduction of T helper cells and regulatory T cells in both spleen and circulation, the hypothesis of cerebral recruitment of these T-cell populations in response to the S1P gradient was investigated. A significant infiltration of $CD45^+$ cells in both hemispheres was revealed, which was particularly characterized by T helper cells.

Fourthly, the S1P receptor ($S1P_R$) expression on leukocytes plays a pivotal role in pIZ recruitment. In this sense, I could demonstrate a significant decrease of $S1P_1$ in the spleen. This result suggested an egress of $S1P_1^+$ immune cells from

the spleen in response to the S1P gradient. In the ischemic hemisphere however, $S1P_1$ mRNA displayed a downregulation, whereas $S1P_2$ and $S1P_3$ showed a significant upregulation. This result might represent sequelae of microglial activation, which is accompanied by an upregulation of $S1P_2$ and $S1P_3$.

Finally, I examined the role of further sphingolipids, i.e., ceramides, which showed a significant increase in the spleen 24 hours after ischemia. In contrast, I could not delineate differences in the brain between the analysed ceramide species, suggesting that a contribution of ceramides to pIZ recruitment is less probable in this model.

In conclusion, the results of this thesis describe a local and systemic involvement of the S1P signaling pathway in immune cell migration after cerebral ischemia. Concordant immune response alterations suggest a relevant role of the changes in sphingolipid concentrations. Further insights into the herein described observations may behold the potential to pave the way to new therapeutic avenues for patients suffering from ischemic stroke.

3. Abkürzungsverzeichnis

Abkürzung	Bedeutung
A. cerebri media	Arteria cerebri media
FoxP3	Forkhead box protein P3
IL-6	Interleukin-6
PIC	Periinfarktkortex
pIZ	Periphere Immunzellen
S1P	Sphingosin-1-Phosphat
$S1P_R$	S1P-Rezeptor
SPI1	Transkriptionsfaktor PU.1
STAT3	Signal transducer and activator of transcription 3

4. Übergreifende Zusammenfassung: Einleitung

4.1. Schlaganfall

Weltweit steht der Schlaganfall an zweiter Stelle der Todesursachenstatistik und stellt eine der Hauptursachen für eine dauerhafte Invalidität und Pflegebedürftigkeit mit gravierenden sozioökonomischen Folgen für die Betroffenen, ihre Angehörigen und die Gesellschaft dar.[1] Weltweit lag die Prävalenz der Schlaganfälle im Jahr 2016 bei 80,1 Millionen, wovon zerebrale Ischämien 84,4% einnahmen.[2] Der akute ischämische Schlaganfall stellt einen medizinischen Notfall dar. Es kommt zu einer akuten Minderperfusion mit einhergehendem neuronalen Funktionsverlust, der mit zunehmender Dauer des Gefäßverschlusses in einem Neuronenuntergang resultiert. Die Ätiologie des ischämischen Schlaganfalls umfasst vornehmlich eine Makroangiopathie der supraaortalen, extra- und intrakraniellen Gefäße, eine zerebrale Mikroangiopathie sowie proximale Emboliequellen. Anamnestisch lässt sich ein apoplektiform aufgetretenes fokal-neurologisches Defizit eruieren. Mangels klinischer Unterscheidungsmerkmale zum hämorrhagischen Schlaganfall in der Prähospitalphase bedarf es einer unverzüglichen Einweisung des Patienten in ein qualifiziertes Schlaganfallzentrum zur weiteren Diagnostik und Therapie.

4.2. Akuttherapien

Oberstes Ziel in der Schlaganfalltherapie ist eine sichere, rapide und effektive arterielle Rekanalisation, um den Blutfluss wiederherzustellen und das funktionelle Outcome zu verbessern.[3,4] Aktuelle Therapieansätze beim ischämischen Schlaganfall stellen die systemische thrombolytische Therapie mit dem intravenös applizierten rekombinanten Gewebeplasminogenaktivator (rtPA) in einem engen Zeitfenster und die endovaskuläre Thrombektomie dar. Verschiedene Studien zeigen eine Überlegenheit der zusätzlichen endovaskulären Therapie gegenüber einer solitären Thrombolyse.[5–12]

Dabei ist das Auftreten einer symptomatischen intrazerebralen Blutung (sICH) nach Thrombolyse und Thrombektomie womöglich nicht allein auf die induzierte Koagulopathie zurückzuführen.[13] Vielmehr zeigen immer mehr Studien, dass die sICH nach Thrombolyse zum Teil mit der postischämischen Neuroinflammation

assoziiert ist.[14–16] Hierbei spielen bei kompromittierter Blut-Hirn-Schranke die Infiltration pIZ, die gliale Aktivierung sowie die Infiltration inflammatorischer Faktoren eine große Rolle.[16,17] Eine kürzlich veröffentlichte Studie hat jedoch auch auf die potentiellen Komplikationen einer mechanischen Thrombektomie mit dem Risiko einer sICH verwiesen.[18]

Eine Option zur Behandlung von Hirninfarktpatienten im Sinne einer medikamentösen Neuroprotektion besteht derzeit noch nicht. Viele Substanzen konnten lediglich im Tiermodell gute Ergebnisse erzielen. So konnte beispielsweise Nerinetid, ein Peptid, welches am postsynaptischen Dichteprotein-95 ansetzt, in der ESCAPE-NA1 Studie vor endovaskulärer Therapie bei schwerem Schlaganfall keine Wirksamkeit demonstrieren.[19]

Immunmodulatorische Ansätze in der Akutphase verbleiben derzeit Gegenstand intensiver präklinischer und klinischer Forschung, solange die reziproken Interaktionen zwischen Immunsystem und zerebraler Ischämie nicht vollständig verstanden sind.[20] Dabei könnte die nähere Charakterisierung des Periinfarktcortex Mechanismen zum Schutz vor sekundären Schäden nach zerebraler Ischämie beitragen.

4.3. Hämorrhagische Transformation

Die häufigsten Komplikationen nach einem Schlaganfall umfassen einen erhöhten intrakraniellen Druck, Schlaganfallrezidive, Infektionen sowie symptomatische intrazerebrale Blutungen nach Thrombolyse.[21]

Eine hämorrhagische Transformation (HT) stellt eine Komplikation des ischämischen Schlaganfalls dar, die hauptsächlich nach Reperfusion auftritt.[22,23] Studien haben ein ca. zehnfach erhöhtes Risiko der HT nach thrombolytischer Therapie (rtPA) gezeigt.[17,24] Neueste Studien aus China, die keinen Unterschied in den HT-Raten zwischen endovaskulärer Therapie mit und ohne Alteplase demonstrieren, leiten einen Paradigmenwechsel ein. So weisen diese auf die Rekanalisation als wesentlichen Treiber der HT hin.[25] Die Aktivierung von Matrix-Metalloproteasen (MMP)[26–28] sowie schwere Endothelschäden nach Ischämie/Reperfusion kompromittieren die endotheliale Integrität und scheinen die Entstehung von HTs zu begünstigen.[29,30] Nach transienter fokaler zerebraler Ischämie

weist die Blut-Hirn-Schranke eine gesteigerte Durchlässigkeit bereits 25 min nach Reperfusion auf, welche für mehrere Wochen anhält.[31,32]

Studien demonstrieren ein erhöhtes Risiko einer hämorrhagischen Transformation in kardioembolischen Hirninfarkten unter einer Antikoagulation.[33,34] Die Vitamin-K-Antagonisten (Phenprocoumon, Warfarin) haben jahrelang Mittel der Wahl der oralen Antikoagulation zur Schlaganfallprävention dargestellt. Zudem sind Vitamin-K-Antagonisten (VKA) zur Thrombembolieprophylaxe bei künstlichem Herzklappenersatz sowie bei Mitralklappenstenosen indiziert. Dabei hemmen diese die Vitamin-K-abhängige Synthese der Gerinnungsfaktoren II, VII, IX, X in der Leber sowie die regulatorischen Faktoren Protein C und S. Allerdings weisen VKAs viele Nachteile auf, vor allem ein geringes therapeutisches Fenster, die Notwendigkeit regelmäßiger INR-Kontrollen sowie das Risiko intrakranieller Blutungen. Im Mausmodell ließ sich eine Exazerbation der hämorrhagischen Transformation unter Warfarin demonstrieren.[35] Ferner zeigten Patienten unter VKA ein höheres Risiko für eine symptomatische intrazerebrale Blutung (sICH) nach mechanischer Thrombektomie.[36]

Leitliniengerecht stellen die neuen direkten oralen Antikoagulanzien (DOAC) eine Alternative zu den Vitamin-K-Antagonisten dar. Sie bieten ein günstigeres Nutzen-Risiko-Profil und werden somit in der Primär- und Sekundärprophylaxe nach Schlaganfall eingesetzt. Während wir uns bei den VKAs INR-Messungen bedienen, die eine gute Kontrollierbarkeit erlauben, fehlt im klinischen Tag eine adäquate Point-of-care-Diagnostik für die DOACs. Der Doasense-Urintest ermöglicht lediglich eine qualitative DOAC-Bestimmung.[37] Studien demonstrieren eine vergleichbare Rate an spontanen HT unter DOACs im Vergleich zu VKA.[38]

4.4. Sphingolipide – Rolle in der Akutphase nach zerebraler Ischämie

Sphingolipide sind ubiquitär vorkommende Komponenten der Zellmembranen und unmittelbar an Zell-Zell-Kontakten sowie an der parakrinen Informationsübermittlung in Geweben beteiligt.[39] Bisher konnte gezeigt werden, dass diversen Sphingolipiden in Krankheitsprozessen eine bedeutende Rolle zukommt.[40–42] Diese Studien haben die Relevanz des Sphingolipidmetabolismus und die Rolle der Sphingolipide als Signalmoleküle als aussichtsreiches therapeutisches

Ziel unterstrichen. Dabei wurden vor allem Sphingosin-1-phosphat (S1P) sowie den Ceramiden Schlüsselrollen zugesprochen.

So konnte die Bedeutung des Sphingosin-1-Phosphats (S1P) als Liganden des Typ 1 S1P-Rezeptors ($S1P_1$) in der Regulation der Lymphozytenverteilung entlang eines S1P-Gradienten demonstriert werden.[43] Eine Modulation des $S1P_1$-Signalweges wurde daher zunächst in der Transplantationsimmunologie[44,45] und später in der Behandlung der neurologischen Autoimmunerkrankung Multiple Sklerose erprobt.[46] Das synthetische, funktionell antagonistische S1P-Analogon Fingolimod (FTY720) wurde 2010 zur Therapie der Multiplen Sklerose zugelassen.[46] Das derzeitige Konzept impliziert die Rekrutierung von Immunzellen entlang steiler S1P-Gradienten, indem S1P den $S1P_1$-Rezeptor ligiert, was zu dessen Internalisierung in die Zelle führt.

Im murinen Schlaganfallmodell konnte gezeigt werden, dass Fingolimod vermutlich über diese immunmodulierende Wirkung zu einer verringerten Infarktgröße, einem verbesserten neurologischen Outcome sowie einer verringerten Anzahl infiltrierender neutrophiler Granulozyten sowie Mikroglia in die ischämische Läsion führt.[47] Ferner gelang der Nachweis einer Reduktion der Thromboinflammation in den Mikrokapillaren im Periinfarktareal unter Fingolimod.[48] Voraussetzung für die protektive Wirkung stellt die Phosphorylierung von Fingolimod über die Sphingosinkinase-2 (SphK2) dar.[49] Der Verlust neuroprotektiver Effekte konnte bei SphK2-defizienten Mäusen demonstriert werden, die eine Zunahme der Infarktgröße sowie eine Zunahme funktioneller neurologischer Defizite aufwiesen.[49]

Ceramide nehmen als Vorläufer des Signalmoleküls S1P eine zentrale Stellung innerhalb des Sphingolipidmetabolismus ein[50] und sind an der Regulation der Apoptose sowie der Zellalterung beteiligt.[51,52] Ferner konnte in Tiermodellen des Schlaganfalls eine Zunahme der Ceramid-Synthese über eine gesteigerte Aktivität der sauren Sphingomyelinase (ASMase) gezeigt werden.[53–56] ASMase-defiziente Mäuse wiesen eine verringerte Infarktgröße und ein verbessertes neurologisches Defizit nach transienter fokaler zerebraler Ischämie auf.[57]

Als Trigger der gesteigerten Ceramidsynthese im Kontext der zerebralen Ischämie wird die induzierte Reperfusion angesehen.[58] Dabei gelten Ceramide als Mediator der Apoptose durch eine mitochondriale Dysfunktion.[59] Zudem wurden

hohe Ceramidspiegel als potentieller gemeinsamer Nenner der Neuroinflammation in neurodegenerativen Erkrankungen tituliert.[60]

4.5. Einfluss der Sphingolipide auf die hämorrhagische Transformation

Erythrozyten sowie Endothelzellen sind die wesentlichen Quellen von S1P und tragen zu einem steilen S1P-Gradienten zwischen dem Blutkompartiment und dem Interstitium bei, wo tausendfach niedrigere S1P-Konzentrationen herrschen. S1P liegt im Plasma entweder an Albumin oder Apolipoprotein M (apoM) gebunden vor.[61–66]

Dabei nimmt $S1P_2$ eine große Rolle in der zerebrovaskulären Integrität ein.[67] In einem Modell der spontanen HT konnte gezeigt werden, dass eine Inhibition von $S1P_2$ die Entwicklung einer HT blockiert.[67]

Studien haben auf die Reduktion einer HT nach Ischämie/Reperfusion unter Fingolimod hingewiesen.[68,69] Im Rahmen der pathophysiologischen Einordnung deuten die Daten von Salas-Perdomo et al. auf einen Lymphozyten-unabhängigen Mechanismus, da Fingolimod auch in Lymphozyten-defizienten Tieren zu einem verringerten Blutungsausmaß sowie einem verbesserten funktionellen Outcome geführt hat.[69] Ferner demonstrierten Studien, dass eine selektive $S1P_1$-Modulation protektive Wirkungen nach intrazerebraler Blutung aufweist.[70] Somit rückt die direkte Wirkung von Fingolimod auf den Sphingolipidmechanismus in den Vordergrund und scheint somit eine hohe translationale Relevanz in der Schlaganfallforschung einzunehmen.

4.6. Darstellung des Manuskripts

Die Studie stellt die Kinetik von Sphingosin-1-phosphat (S1P) in der Akutphase der fokalen zerebralen Ischämie sowie die damit einhergehenden systemischen Veränderungen von T-Helferzellen (T_H-Zellen) und regulatorischen T_H-Zellen (T_{REG}-Zellen) als wichtige Akteure des Immunsystems dar. Hier konnte ich demonstrieren, dass ein steiler S1P-Gradient von der Milz in Richtung Gehirn vorherrschend war. Mittels quantitativer PCR (qPCR) schien der $S1P_1^+$ der prädominierend aus der Milz austretenden Zellphänotyp zu sein. Ferner konnte ich

nachweisen, dass die Rekrutierung T_H- und T_{REG}-Zellen in die ischämische Hemisphäre mit einer differentiellen Regulation des $S1P_R$-Expressionsmusters assoziiert ist.

Um die Rolle von S1P als chemotaktisches Agens im Kontext der zerebralen Ischämie näher zu charakterisieren, erfolgte zunächst die Bestimmung von S1P in verschiedenen Kompartimenten (Milz, Plasma, Gehirn). Hierzu wurde ein C57BL/6 Tiermodell der fokalen zerebralen Ischämie (mittels Fadenokklusion der Arteria cerebri media, *MCAO*) verwendet. Letztere resultierte in einer Hochregulation des S1P-Signalwegs und einem Anstieg des S1P-Spiegels in der ischämischen Hemisphäre sowie im Plasma nach 24 Stunden. Eine in unserer Arbeitsgruppe durchgeführte Beobachtungsstudie an Patienten ergab ebenso einen signifikanten Anstieg des S1P-Spiegels im Plasma innerhalb von 24 Stunden nach Schlaganfall. Dagegen ließ sich drei Stunden nach Ischämie eine Reduktion von S1P sowohl im ischämischen murinen Kortex, als auch im Periinfarktkortex (PIC) nachweisen. Die Reduktion der S1P-Spiegel im PIC persistierte bis 24 Stunden nach Induktion der Ischämie. Somit etablierte dies einen neuen S1P-Gradienten zwischen dem ischämischen Kern ($S1P^{HIGH}$) und dem PIC ($S1P^{LOW}$). In der Milz konnte eine Reduktion von S1P 24 Stunden nach MCAO demonstriert werden.

Aufgrund der Bedeutung von S1P in der Rekrutierung von Immunzellen habe ich im Folgenden eine mögliche Korrelation zwischen der S1P-$S1P_R$-Achse und der Immunzellenrekrutierung in der Akutphase nach fokaler zerebraler Ischämie untersucht. Durchflusszytometrische Analysen zeigten hierbei eine signifikante Abnahme der B- und T-Lymphozyten in der Milz 24 Stunden nach MCAO. Makroskopisch ließ sich dabei eine deutliche Atrophie der postischämischen Milz abgrenzen.

Analog zu den Veränderungen in der Milz konnte auch in der Zirkulation eine Reduktion der B- und T-Zellen 24 Stunden nach fokaler zerebraler Ischämie nachgewiesen werden. Angesichts des S1P-Gradienten stellten wir die Hypothese einer Rekrutierung dieser T-Zell-Populationen in Richtung der dominierenden S1P-Konzentration in der ischämischen Hemisphäre auf. Dabei gelang die Darstellung einer signifikanten Infiltration $CD45^+$-Zellen, welche insbesondere T_H-Zellen entsprach.

Ausgehend von unseren experimentellen Befunden sowie zur näheren Untersuchung der Chemotaxis von Immunzellen angesichts hoher S1P-Spiegel nach zerebraler Ischämie erfolgte die nähere Charakterisierung der $S1P_R$-Expression in splenischen Immunzellen. Dabei konnte ich eine signifikante Reduktion der $S1P_1$ mRNA-Konzentrationen 24 Stunden nach MCAO nachweisen. Dagegen ließen sich keine signifikanten Änderungen der $S1P_2$, $S1P_3$ und $S1P_4$ mRNA-Konzentrationen abgrenzen.

In der ischämischen Hemisphäre imponierte eine geringere $S1P_1$-mRNA-Konzentration, während die $S1P_2$- und $S1P_3$-mRNA-Konzentrationen gesteigert waren. Mittels immunhistochemischer Färbungen konnte eine Akkumulation von $CD3^+$ und $FoxP3^+$ Zellen vor allem im Periinfarktcortex nachgewiesen werden.

Ferner erfolgte die Bestimmung der Ceramide in der Milz nach fokaler zerebraler Ischämie, die einen signifikanten Anstieg 24 Stunden nach fokaler zerebraler Ischämie zeigten. Dagegen ließen sich im Gehirn keine signifikanten Unterschiede der Ceramide abgrenzen.

4.7. Diskussion der Gesamtheit der Ergebnisse

Der Sphingolipid-Signalweg stellt ein aussichtsreiches Ziel pharmakologischer Interventionen in der Schlaganfalltherapie dar. S1P gilt als Signalmolekül und ist an der Regulation immunologischer Prozesse beteiligt.[39,71] Die S1P-Konzentration wird von den Sphingosinkinasen 1 (SphK1) und 2 (SphK2) beeinflusst.[72] Es besteht ein steiler S1P-Konzentrationsgradient zwischen dem Gefäßkompartiment und dem Interstitium, wo niedrige nanomolare Konzentrationen herrschen. Vor allem Erythrozyten und Endothelzellen gelten als wesentliche Quellen von S1P[66]. Es wurde postuliert, dass S1P die Lymphozytenverteilung im Organismus entlang eines S1P-Gradienten reguliert.[73,74] So führt Fingolimod, ein synthetisches, funktionell antagonistisches S1P-Analogon, welches bei der Autoimmunerkrankung Multiple Sklerose Anwendung findet, zu einer Lymphozytensequestrierung in die Lymphknoten vermittelt durch die Internalisierung von $S1P_1$.[75]

Wir konnten einen steilen S1P-Gradienten zum ischämischen Kern nachweisen, während S1P im Periinfarktcortex eine Reduktion aufwies. Hasegawa et al. haben zwar eine Reduktion von $S1P_1$, SphK1 und SphK2 im Infarktcortex nachgewiesen, im Periinfarktcortex zeigten sich diese jedoch für mindestens 6 Stunden

nach MCAO stabil.[76] Die Exposition von S1P an $S1P_1$ führt zur Liganden-induzierten Internalisierung des $S1P_1$ Rezeptors.[65] Somit besagt die von uns verfolgte Hypothese, dass die nachgewiesenen niedrigeren S1P-Spiegel in der Penumbra eine verminderte Internalisierung des Rezeptors im Sinne einer negativen Rückkopplungsschleife der S1P-Ligation an $S1P_1$ induzieren. Dies resultiert in einer erhaltenen Expression von $S1P_1$ und aktiver SphK1/2.[65] Als Voraussetzungen für den Lymphozytenaustritt aus sekundär lymphatischen Organen gelten ein intakter, chemotaktischer Gradient sowie die $S1P_1$-Expression.[74,77] Eine anhaltende Exposition von S1P an $S1P_1$ resultiert in einem verminderten Ansprechen der $S1P_1$-mediierten Chemotaxis. In SphK-defizienten Mäusen ließen sich auf Lymphozyten eine hohe Expression von $S1P_1$ im Vergleich zu Kontrollen nachweisen, konkordant mit einem Mangel an zirkulierendem S1P.[65]

Studien habe ferner gezeigt, dass Populationen von T_H- sowie T_{REG}-Zellen bereits am ersten Tag in der ischämischen Hemisphäre akkumulieren.[78–80] Diese Daten decken sich mit unseren qPCR und immunhistochemischen Ergebnissen. Zudem stellen Neurone eine mögliche S1P-Quelle dar, da das Gehirn die höchsten S1P-Konzentrationen aufweist,[81] sodass der durch die fokale zerebrale Ischämie induzierte Neuronenuntergang zu einem Austritt von S1P in den ischämischen Kern führen könnte. Dies wiederum würde einen neuen S1P-Gradienten etablieren, der das Einwandern von Immunzellen in den Periinfarktcortex begünstigen könnte.

Die differentielle Lokalisation und Konzentration der verschiedenen $S1P_R$ auf der Zelloberfläche entscheiden über die Wirkung von S1P.[77,82] So nehmen auch $S1P_2$ und $S1P_3$ eine wichtige Rolle in der Lymphozytenmigration ein.[83–86] $S1P_2$ wird von vaskulären Endothelzellen exprimiert und spielt eine wichtige Rolle in der vaskulären Permeabilität und Inflammation.[87,88] Dagegen wird $S1P_3$ auf embryonalen Endothelzellen exprimiert und agiert als Mediator P-Selektin-mobilisierender Effekte über die Aktivierung von SphK1[84–86,89]. Ferner moduliert $S1P_3$ die mikrogliale Aktivierung sowie die M1-Polarisation im Kontext der zerebralen Ischämie.[90] In dieser Arbeit konnte ich eine Erhöhung der $S1P_3$-mRNA in der ipsilateralen Hemisphäre nach fokaler zerebraler Ischämie nachweisen, die mit einer gesteigerten CD3- und FoxP3-Expression einherging.

Es fanden sich höhere S1P-Spiegel in der Zirkulation nach MCAO, die zu einem verstärkten Austritt von Lymphozyten aus der Milz nach der Ischämie beigetragen haben könnten. Bereits drei Stunden nach MCAO war eine Abnahme der Lymphozyten in der Zirkulation nachweisbar. Daher stellt die Migration von Immunzellen einen Prozess dar, der sich in engmaschiger zeitlicher Abfolge unmittelbar nach MCAO abspielt.[78–80] Hier gilt es zu beleuchten, inwieweit die Expression von $S1P_{1-5}$ oder anderer Glykosphingolipide wie Ceramide die Chemotaxis von Immunzellen zum Gehirn fördern/mediieren könnte.

Während ich in der Milz nach MCAO erhöhte Ceramid-Spiegel nachweisen konnte, die am ehesten auf die koinzidentelle Apoptose zurückzuführen waren, ließen sich im Periinfarktkortex keine signifikanten Veränderungen von Ceramiden abgrenzen.

4.8. Deren Beitrag/Bedeutung für die Beantwortung der Fragestellung

Unsere Ergebnisse weisen auf eine relevante Rolle von S1P im Kontext der zerebralen Ischämie und der damit assoziierten Immunzellrekrutierung hin. Die Literatur zeigt eine Akkumulation von S1P im Infarktkern, die Kimura et al. auf Mikroglia und Astrozyten als S1P-Quellen zurückgeführt haben.[83] Salas-Perdomo et al. gelang der Nachweis einer Hochregulation der SphK1-mRNA nach Ischämie und damit einhergehend der S1P-Konzentration.[69] Angesichts der übergeordneten Stellung von S1P in der Chemotaxis von T-Zellen wurde von den Autoren eine Assoziation zwischen der gesteigerten S1P-Konzentration und der erhöhten Anzahl $S1P_1^+$-T-Zellen in der ipsilateralen Hemisphäre postuliert.[69] Diese Arbeiten unterstützen unsere Ergebnisse.

Für die durch S1P-vermittelte Chemotaxis ist ein etablierter S1P-Gradient und die Expression von $S1P_1$ von Bedeutung, um Lymphozyten aus sekundär lymphatischen Organen zu rekrutieren.[74,77] So konnte meine Arbeit $S1P_1^+$-Zellen als wesentliche Population nachweisen, welche die Milz verlassen hatten. Durchflusszytometrische Analysen zeigten dabei eine signifikante Abnahme der B- und T-Lymphozyten in der Milz im Einklang mit dem histologischen Nachweis der Reduktion der weißen Pulpa 24 Stunden nach MCAO. Ferner konnte eine Abnahme der T-Helferzellen sowie regulatorischer T-Zellen sowohl in der Milz als auch in der Zirkulation nachgewiesen werden. Wir nahmen eine Akkumulation dieser T-

Zellpopulationen anhand des S1P-Gradienten im Gehirn an. Hierzu passend konnten Malone et al., 2021 eine Zunahme der FoxP3^{+} Zellen in der infarzierten Hemisphäre nachweisen.[91] Die Migration peripherer Immunzellen ins zentrale Nervensystem mit anschließender Infiltration ins ischämische Hirnparenchym wird als potentieller Mechanismus einer Potenzierung der Schädigung von Hirngewebe angesehen. Dabei weisen Studien auf die Schlüsselrolle infiltrierender T-Zellen ins zentrale Nervensystem hin.[92,93]

Zusammenfassend stellt der Sphingolipid-Signalweg ein aussichtsreiches Ziel pharmakologischer Interventionen in der Schlaganfalltherapie dar.

5. Übersicht der Publikation

Lucaciu A, Kuhn H, Trautmann S, S., Ferreirós, N., Steinmetz, H., Pfeilschifter, J., Brunkhorst, R., Pfeilschifter, W., Subburayalu, J., & Vutukuri, R. A Sphingosine 1-Phosphate Gradient Is Linked to the Cerebral Recruitment of T Helper and Regulatory T Helper Cells during Acute Ischemic Stroke. *Int J Mol Sci*. 2020;21(17):6242. Published 2020 Aug 28. doi:10.3390/ijms21176242

6. Publikation

International Journal of *Molecular Sciences*

MDPI

Article

A Sphingosine 1-Phosphate Gradient Is Linked to the Cerebral Recruitment of T Helper and Regulatory T Helper Cells during Acute Ischemic Stroke

Alexandra Lucaciu [1,*], Hannah Kuhn [1], Sandra Trautmann [2], Nerea Ferreirós [2], Helmuth Steinmetz [1], Josef Pfeilschifter [3], Robert Brunkhorst [1,4], Waltraud Pfeilschifter [1], Julien Subburayalu [5,†] and Rajkumar Vutukuri [3,*,†]

1 Department of Neurology, Goethe University Frankfurt, 60528 Frankfurt am Main, Germany; hannah.kuhn@gmail.com (H.K.); h.steinmetz@em.uni-frankfurt.de (H.S.); rbrunkhorst@ukaachen.de (R.B.); waltraud.pfeilschifter@kgu.de (W.P.)
2 Institute of Clinical Pharmacology, Pharmazentrum Frankfurt, Goethe University Frankfurt, 60528 Frankfurt am Main, Germany; trautmann@med.uni-frankfurt.de (S.T.); ferreirosbouzas@em.uni-frankfurt.de (N.F.)
3 Institute of General Pharmacology and Toxicology, Pharmazentrum Frankfurt, Goethe University Frankfurt, 60528 Frankfurt am Main, Germany; pfeilschifter@em.uni-frankfurt.de
4 Department of Neurology, RWTH Aachen University, 52074 Aachen, Germany
5 Department of Medicine, University of Cambridge, Cambridge CB2 0QQ, UK; js2380@cam.ac.uk
* Correspondence: alexandra.lucaciu@kgu.de (A.L.); vutukuri@med.uni-frankfurt.de (R.V.)
† These authors contributed equally.

Received: 7 July 2020; Accepted: 26 August 2020; Published: 28 August 2020

check for updates

Abstract: Emerging evidence suggests a complex relationship between sphingosine 1-phosphate (S1P) signaling and stroke. Here, we show the kinetics of S1P in the acute phase of ischemic stroke and highlight accompanying changes in immune cells and S1P receptors ($S1P_R$). Using a C57BL/6 mouse model of middle cerebral artery occlusion (MCAO), we assessed S1P concentrations in the brain, plasma, and spleen. We found a steep S1P gradient from the spleen towards the brain. Results obtained by qPCR suggested that cells expressing the $S1P_R$ type 1 ($S1P_1{}^+$) were the predominant population deserting the spleen. Here, we report the cerebral recruitment of T helper (T_H) and regulatory T (T_{REG}) cells to the ipsilateral hemisphere, which was associated with differential regulation of cerebral $S1P_R$ expression patterns in the brain after MCAO. This study provides insight that the S1P-$S1P_R$ axis facilitates splenic T cell egress and is linked to the cerebral recruitment of $S1P_R{}^+$ T_H and T_{REG} cells. Further insights by which means the S1P-$S1P_R$-axis orchestrates neuronal positioning may offer new therapeutic perspectives after ischemic stroke.

Keywords: sphingosine 1-phosphate; regulatory T helper cells; stroke; sphingosine kinase; sphingosine 1-phosphate receptor; ceramides; fingolimod

1. Introduction

In the last two decades, the formerly enigmatic sphingolipids and their metabolism have aroused a lot of biomedical research interest due to their pivotal role as signaling molecules. The regulation of a wide range of cellular processes was described, including endocytosis, intracellular trafficking of molecular constituents, and signal transduction by membrane receptors [1,2]. Recent insights into the molecular mechanisms of action provide increasing evidence for the complex pathways of sphingolipid metabolism in the pathogenesis of multiple diseases including cancer, diabetes, neurodegenerative disorders, autoimmune diseases, and stroke [3–7]. Fingolimod represents an

unselective functional antagonist to sphingosine 1-phosphate receptors ($S1P_R$) resulting in $S1P_R$ downregulation upon $S1P_R$ engagement [8,9]. The successful application of fingolimod in the treatment of various diseases characterized by a perturbed S1P metabolism suggests the strong therapeutic potential of the S1P-$S1P_R$-axis [8,10–12].

To date, S1P is conceived to regulate immune cell recruitment towards high S1P gradients [13,14] by ligating the five bona fide $S1P_R$ type 1–5 ($S1P_{1–5}$) [15]. This gradient is perturbed under diseased conditions and $S1P_R$ signaling acts as a driver of multiple diseases [16]. However, how the S1P-$S1P_R$-axis contributes to pathology in focal cerebral ischemia has not been elucidated in all details [17–19].

Ischemic stroke holds a high mortality [20] and its treatment is currently limited to restoring the impaired blood flow [21]. Moreover, neuroprotectants have failed to add on currently available therapeutic options [22]. In contrast, characterizing the dysfunction and elucidating the mechanism of recovery in the peri-infarct cortex, i.e., the non-ischemic tissue surrounding the ischemic core, may possess therapeutic potential and protect from delayed secondary damage after ischemic stroke [23]. In that respect, fingolimod has been shown to improve outcome after stroke in preclinical and clinical trials [5,6,24,25].

The first well-characterized biological effects of S1P signaling were described in immune cells [26], demonstrating a key role of S1P and $S1P_R$ ligation in regulating T cell distribution [9,14]. In stroke research, evidence has accumulated that focal cerebral ischemia facilitates an acute inflammatory cascade characterized by the infiltration of inflammatory cells and, in particular, T cells in an early and antigen-independent manner into the ischemic brain to contribute to post-ischemic brain damage [27–29]. The detrimental impact of lymphocyte infiltration in early ischemic brain injury led by T and B lymphocytes as injurious players was shown in experimental stroke by T and B cell-deficient mice (SCID) [30], as well as asplenic rats [31]. In addition, studies suggest a dynamical reflection in the peripheral immune system [32], leading to a state of immunosuppression. A better characterization of the migration of immune cells into the ischemic cerebral parenchyma represents a prerequisite for therapeutic interventions [33].

Therefore, the aims of this study were to unravel the kinetics of the S1P metabolism and the differential regulation of $S1P_R$ on systemic alterations of immune cell populations with reference to their cerebral recruitment in the acute phase of ischemic stroke. Understanding the mechanisms by which immune cell subsets are recruited to the brain via S1P could widen therapeutic options in ischemic stroke.

2. Results

2.1. Acute Ischemic Stroke Leads to Increased Plasma S1P Levels and Creates a Gradient between the Ischemic Core and the Peri-Infarct Cortex

In order to study the potential of S1P to act as a chemotactic agent in cerebral ischemia, we established a temporal profile of S1P concentrations in the murine spleen, plasma, and brain in a model of acute cerebral ischemia (MCAO). Under homeostasis, a steep S1P gradient exists towards the brain with the lowest concentration found in the spleen and a moderate concentration observed in the plasma (Figure 1A). In the plasma, a significant S1P increase was observed 24 h after stroke (sham vs. MCAO; 352.8 ± 20.0 ng/mL vs. 482.4 ± 55.0 ng/mL, $p < 0.0001$, Figure 1A). Prior to 24 h, no significant change could be reported both at 3 h (sham vs. MCAO; 352.8 ± 20.0 ng/mL vs. 327.5 ± 35.9 ng/mL, $p = 0.168$, Figure 1A) and 12 h after MCAO (sham vs. MCAO; 352.8 ± 20.0 ng/mL vs. 375.6 ± 61.3 ng/mL, $p = 0.3056$, Figure 1A). In humans, who had suffered from acute ischemic stroke (Str), we were able to measure similar changes 24 h after onset of ischemia as compared to healthy controls (C) (C vs. Str; 4.55 ± 2.1 ng/mg vs. 6.53 ± 5.0 ng/mg, $p = 0.0034$, Figure 1B).

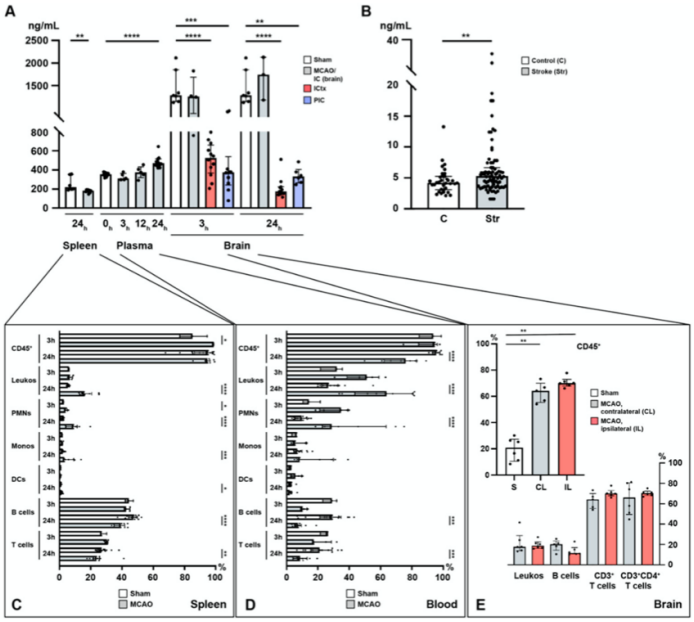

Figure 1. Temporal profile of immuno-cellular and sphingosine 1-phosphate (S1P) alterations after acute ischemic stroke in the spleen, circulation, and the brain. (**A**) Murine S1P levels are shown in the spleen (24 h), the plasma (3, 12, and 24 h), and the brain (3 and 24 h) after MCAO. (**B**) Enhanced S1P plasma levels in patients with ischemic stroke. (**C**) Alterations in immune cell populations in the murine spleen (3 and 24 h) after middle cerebral artery occlusion (MCAO). (**D**) Alterations in immune cell populations in the murine blood (3 and 24 h) after MCAO. (**E**) $CD45^+$ pan-immune cells are expanded in the murine brain 24 h after MCAO. The vast majority of these $CD45^+$ cells comprised T cells. IC: ischemic core; ICtx: ischemic cortex; PIC: peri-infarct cortex. The Mann–Whitney U-test was applied to calculate statistical differences, except for the mouse plasma data (Kruskal–Wallis test) and for the human stroke samples (unpaired t test with Welch's correction). The data are presented as median ± IQR; * $p < 0.05$, ** $p < 0.01$, *** $p < 0.001$, **** $p < 0.0001$.

In the brain, S1P remains high in the ischemic core (IC) with a tendency to further increase within the first 24 h, although statistical significance could not be reached due to a small sample size (3 h: sham vs. MCAO; 1448 ± 380.4 pg/mg vs. 1275 ± 435.4 pg/mg, $p = 0.4121$, Figure 1A; 24 h: sham vs. MCAO; 1448 ± 380.4 pg/mg vs. 1685 ± 477.8 pg/mg, $p = 0.5167$, Figure 1A; IC_{3h} vs. IC_{24h}; 1275.0 ± 435.4 vs. 1685.0 ± 477.8, $p = 0.6286$, Figure 1A). In contrast, S1P was reduced 3 h after the MCAO challenge had occurred in the peri-infarct cortex (PIC) (sham vs. MCAO; 1448 ± 380.4 pg/mg vs. 425.0 ± 284.8 pg/mg, $p = 0.0001$, Figure 1A), as well as in the ischemic cortex (ICtx) (sham vs. MCAO; 1448 ± 380.4 pg/mg vs. 509.0 ± 180.4 pg/mg, $p < 0.0001$, Figure 1A) compared to the corresponding cortex in sham-operated mice. The reduction in S1P levels in the PIC persisted over 24 h (sham vs. MCAO; 1448 ± 380.4 pg/mg vs. 340.6 ± 85.2 pg/mg, $p = 0.0012$, Figure 1A) but was unchanged compared to 3 h after MCAO (PIC_{3h} vs. PIC_{24h}; 425.0 ± 284.8 vs. 340.6 ± 85.2, $p = 0.6159$, Figure 1A). This reduction allowed a new S1P gradient to be established between the IC and the PIC (3 h: IC vs. PIC; 1275.0 ± 435.4 vs. 425.0 ± 284.8, $p = 0.007$, Figure 1A), which even steepened at 24 h (24 h: IC vs. PIC; 1685.0 ± 477.8 vs. 340.6 ± 85.2, $p = 0.0238$, Figure 1A). The decrease in the ICtx also prevailed at 24 h (sham vs. MCAO;

1448 ± 380.4 pg/mg vs. 210.8 ± 109.2 pg/mg, $p < 0.0001$, Figure 1A) and consolidated ($ICtx_{3h}$ vs. $ICtx_{24h}$; 509.0 ± 180.4 vs. 210.8 ± 109.2, $p = 0.0002$, Figure 1A).

In the spleen, S1P was reduced 24 h after MCAO (sham vs. MCAO; 256.5 ± 77.9 pg/mg vs. 178.5 ± 16.0, $p = 0.0027$, Figure 1A).

2.2. Lymphocyte Evasion from the Spleen after Acute Ischemic Stroke

Next, we assessed the immune cell traffic between these compartments in the context of stroke. Our data suggest an evasion of splenic lymphocytes (T and B cells) and a striking regulation of all leukocyte populations in the circulation (blood). As an established surrogate marker for immune cell egress, the spleen weight was evaluated after MCAO (Figure S1) yielding a relevant reduction in splenic weight as early as 12 h after MCAO (sham vs. MCAO; 70.0 ± 12.3 mg vs. 50.0 ± 7.1 mg, $p = 0.0238$, Figure S1). This reduction was even more pronounced 24 h after MCAO (sham vs. MCAO; 80.0 ± 19.1 mg vs. 48.3 ± 8.3 mg, $p < 0.0001$, Figure S1).

Flow cytometric analysis of spleen homogenates revealed relevant changes in terms of decreasing relative cell numbers in B and T cells, although this change took 24 h in our study to reach statistical significance. Here, B cell frequencies remained unchanged at 3 h (sham vs. MCAO; 44.6 ± 2.5 vs. 43.1 ± 1.9, $p = 0.57$, Figure 1C) and decreased at 24 h (sham vs. MCAO; 46.6 ± 3.9 vs. 39.0 ± 3.5, $p < 0.0001$, Figure 1C). Similarly, at 3 h no change was observed in T cells (sham vs. MCAO; 27.9 ± 2.0 vs. 30.1 ± 1.1, $p = 0.1429$, Figure 1C), whilst a reduction was detected at 24 h (sham vs. MCAO; 27.7 ± 3.8 vs. 24.7 ± 6.1, $p = 0.0093$, Figure 1C). Additionally, we measured the pro-inflammatory IL-6 (a pleiotropic cytokine), and the transcription factors (TFs) SPI1 (B cell TF), STAT3 (T_H cells), and FoxP3 (T_{REG} cells) (Figure S2). Indeed, we found severe alterations in the expression level of IL-6 at 3 and 24 h after MCAO suggesting pan-immune cell egress (3 h: sham vs. MCAO; 1.0 ± 0.4 vs. 0.0 ± 0.0, $p = 0.0005$; 24 h: sham vs. MCAO: 1.0 ± 0.4 vs. 0.2 ± 0.1, $p < 0.0001$, Figure S2). In terms of specific cell populations, we measured SPI1, which suggested early B cell egress from the spleen at 3 h (sham vs. MCAO; 1.0 ± 0.2 vs. 0.3 ± 0.1, $p = 0.001$, Figure S2). In contrast, these effects were revoked as indicated by levels of SPI1 at 24 h comparable to sham (sham vs. MCAO; 1.0 ± 0.2 vs. 1.1 ± 0.3, $p = 0.2775$, Figure S2). Unlike B cells, T_H and T_{REG} cells remained reduced at 3 and 24 h alike, although not statistically significant for T_{REG} cells (T_H cells identified by STAT3: 3 h: sham vs. MCAO; 1.0 ± 0.3 vs. 0.2 ± 0.0, $p = 0.001$; 24 h: sham vs. MCAO; 1.0 ± 0.3 vs. 0.4 ± 0.2, $p = 0.0003$; T_{REG} cells identified by FoxP3: 3 h: sham vs. MCAO; 1.0 ± 0.1 vs. 0.2 ± 0.0, $p = 0.0005$; 24 h: sham vs. MCAO; 1.0 ± 0.1 vs. 0.8 ± 0.8, $p = 0.0652$, Figure S2). Taken together, this hints at reduced numbers of splenic lymphocytes, in accordance with previous reports [32].

By contrast, CD45, which was used as a pan-leukocyte and pan-lymphocyte marker, showed an early increase after 3 h (sham vs. MCAO; 85.6 ± 8.8 vs. 98.6 ± 0.2, $p = 0.036$, Figure 1C). This effect was no longer seen after 24 h (sham vs. MCAO; 91.3 ± 8.7 vs. 94.8 ± 3.7, $p = 0.5197$, Figure 1C). The relative frequencies of leukocytes ($CD45^+CD11b^+$ cells) were unaffected at 3 h (sham vs. MCAO; 6.0 ± 0.4 vs. 7.0 ± 1.4, $p = 0.25$, Figure 1C) and increased after 24 h (sham vs. MCAO; 5.7 ± 0.7 vs. 17.3 ± 4.6, $p < 0.0001$, Figure 1C). Polymorphonuclear neutrophils (PMNs) characterized by the expression of Ly6G in $CD45^+$ cells were increased both at 3 h (sham vs. MCAO; 2.6 ± 0.1 vs. 4.1 ± 1.1, $p = 0.0357$, Figure 1C) and 24 h after MCAO (sham vs. MCAO; 2.1 ± 0.8 vs. 9.2 ± 4.6, $p < 0.0001$). Monocyte frequencies ($CD45^+Ly6C^{MODERATE}$) were only increased after 24 h (3 h: sham vs. MCAO; 1.7 ± 0.2 vs. 1.8 ± 0.5, $p = 0.7857$; 24 h: sham vs. MCAO; 2.1 ± 0.8 vs. 5.3 vs. 4.0, $p = 0.0008$, Figure 1C). Dendritic cells ($CD45^+Ly6C^{HIGH}$) displayed only a subtle change in their frequencies (3 h: sham vs. MCAO; 0.9 ± 0.1 vs. 0.7 ± 0.4, $p = 0.25$; 24 h: sham vs. MCAO; 0.8 ± 0.3 vs. 1.4 ± 0.6, $p = 0.0133$, Figure 1C).

2.3. Immune Cell Alterations in the Circulation after Acute Ischemic Stroke

As in the spleen, significant alterations of immune cell counts could be appreciated in the circulation (Figure 1D). $CD45^+$ cells were reduced in the circulation after 24 h (sham vs. MCAO; 95.5 ± 2.5 vs. 72.9 ± 13.1, $p < 0.0001$), but not at 3 h after MCAO (sham vs. MCAO; 92.3 ± 7.1 vs.

91.1 ± 9.3, $p > 0.9999$, Figure 1D). While the relative numbers of leukocytes increased in the circulation although this effect only reached statistical significance after 24 h (3 h: sham vs. MCAO; 29.8 ± 7.2 vs. 49.3 ± 12.0, $p = 0.1429$; 24 h: sham vs. MCAO; 29.3 ± 9.4 vs. 61.5 ± 18.6, $p < 0.0001$, Figure 1D) and this increase was reflected in neutrophil frequencies, in spite of more pronounced variation compared to the entirety of leukocytes (3 h: sham vs. MCAO; 15.5 ± 5.5 vs. 31.2 ± 9.5, $p = 0.0714$; 24 h: sham vs. MCAO; 9.4 ± 4.0 vs. 39.0 ± 22.2, $p < 0.0001$, Figure 1D), monocytes and dendritic cells remained entirely unaltered (monocytes: 3 h: sham vs. MCAO; 5.5 ± 1.8 vs. 7.9 ± 4.5, $p = 0.9643$; 24 h: sham vs. MCAO; 7.7 ± 4.1 vs. 17.2 ± 13.1, $p = 0.0622$; dendritic cells: 3 h: sham vs. MCAO; 2.3 ± 1.0 vs. 6.1 ± 3.6, $p = 0.2286$; 24 h: sham vs. MCAO; 2.6 ± 1.3 vs. 2.6 ± 1.8, $p = 0.7564$, Figure 1D). Analogous to decreased frequencies observed in the spleen, B and T cells were also reduced in the circulation after 24 h (B cells: 3 h: sham vs. MCAO; 28.1 ± 4.5 vs. 10.8 ± 2.2, $p = 0.0571$; 24 h: sham vs. MCAO; 27.1 ± 11.4 vs. 8.2 ± 4.6, $p = 0.0004$; T cells: 3 h: sham vs. MCAO; 24.7 ± 2.7 vs. 21.7 ± 6.7, $p = 0.3929$; 24 h: sham vs. MCAO; 21.7 ± 8.4 vs. 9.4 ± 5.3, $p = 0.0007$, Figure 1D).

2.4. Sphingosine 1-Phosphate Is Linked to Cerebral T Cell Recruitment after Acute Ischemic Stroke

Given the S1P gradient found and the decreased frequency of T_H and T_{REG} cells both in the spleen and circulation alike, we assumed these T cell populations would be subject to a swift recruitment towards the high S1P concentration present in the brain, which was particularly high in the IC after stroke. The release and migration of peripheral immune cells into the central nervous system (CNS) with subsequent infiltration into the ischemic brain parenchyma are conceived as a putative mechanism to potentiate brain damage [34,35]. We found that $CD45^+$ immune cells were recruited to the brain 24 h after MCAO as indicated by a significant increase of $CD45^+$ immune cell frequencies (Figure 1E). Here, a recruitment of $CD45^+$ cells was observed to the contralateral hemisphere (CL) (sham vs. CL; 19.6 ± 8.8 vs. 63.0 ± 7.8, $p = 0.0043$, Figure 1E) and to the ipsilateral hemisphere (IL) (sham vs. IL; 19.6 ± 8.8 vs. 70.6 ± 4.0, $p = 0.0022$, Figure 1E), although no difference between the CL and the IL could be established (CL vs. IL; 63.0 ± 7.8 vs. 70.6 ± 4.0, $p = 0.1875$, Figure 1E). Of interest, the vast majority of these infiltrating immune cells comprised T_H cells ($CD3^+$: CL vs. IL; 63.0 ± 7.8 vs. 70.6 ± 4.0; $CD3^+CD4^+$: CL vs. IL; 64.9 ± 15.7 vs. 70.4 ± 2.9, Figure 1E). In contrast, non-lymphocytic leukocytes and B cells contributed only scarcely to the $CD45^+$ immune cell recruitment observed (leukocytes: CL vs. IL; 21.4 ± 10.6 vs. 19.7 ± 4.2; B cells: CL vs. IL; 19.1 ± 5.5 vs. 13.7 ± 4.8, Figure 1E).

In appreciation of these findings and in light of the S1P gradient measured we investigated the kinetics of $S1P_R$ expression in the spleen and brain after acute ischemic stroke.

2.5. $S1P_1$ Might Contribute to the Lymphocyte Evasion from the Spleen after Acute Ischemic Stroke

To evaluate the putative mechanism behind the chemotaxis of immune cells in light of the increasing S1P plasma levels after stroke, the relationship of $S1P_R$ expression between immune cells deserting the spleen and the central nervous system (CNS) was analyzed. In this regard, it was previously postulated that splenic responses after stroke and their contribution to ischemic brain damage represent important players in the pathology underlying stroke [36]. Our findings that the spleen is subject to drastic shrinkage during the acute phase after MCAO (Figure 2A), are in accordance with previous reports [31,32]. In addition, histopathology of spleens 24 h after MCAO displayed a predominant reduction of the lymphoid tissue, in particular, and to some subtler extent hematopoietic elements in the red pulp (Figure 2B,C). Previous studies have highlighted the importance of S1P receptor expression by various immune cells, and T and B cells in particular, for lymphocyte egress from tissues [37]. Hence, we measured the $S1P_R$ mRNA expression after MCAO from splenic tissue lysates. We detected a significant reduction in the mRNA levels of $S1P_1$ 24 h after MCAO (sham vs. MCAO; 1.00 ± 0.2 vs. 0.5 ± 0.1, $p = 0.0002$, Figure 2D). To test $S1P_1$-specificity of this phenomenon, we measured mRNA levels of $S1P_2$, $S1P_3$, and $S1P_4$ and did not find any significant alterations ($S1P_2$: undetermined (UD) in sham vs. MCAO; $S1P_3$: sham vs. MCAO; 1.0 ± 0.2 vs. 1.0 ± 0.3, $p = 0.8968$; $S1P_4$: sham vs. MCAO; 1.0 ± 0.2 vs. 0.8 ± 0.3, $p = 0.1903$, Figure 2D). These findings suggest predominantly

$S1P_1^+$-immune cells to evade the spleen in response to the S1P gradient towards the brain secondary to an additional trigger set off by cerebral ischemia. $S1P_1$ is conceived to play an important role in T cell egress from secondary lymphoid organs towards high S1P gradients [38,39]. Given that only B cells and T cells were present at lower frequencies in the spleen after ischemic stroke (Figure 1C), we assume that the expression of $S1P_1$ may be required for their evasion from the spleen.

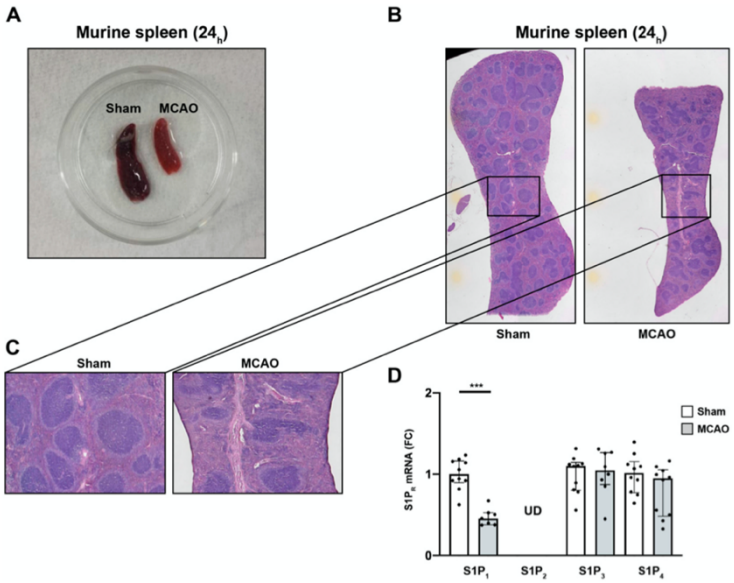

Figure 2. $S1P_1$ immune cell egress from the spleen after acute ischemic stroke. (**A**) Macroscopic reduction in spleen size 24 h after MCAO (sham-(left) vs. MCAO-operated mice (right)). (**B**) Microscopic comparison of sham-(left) vs. MCAO-treated mice (right). (**C**) Inserts display a predominant reduction of white pulp tissue compared to the red pulp, which was only mildly affected. (**D**) Detection of $S1P_1$, $S1P_2$, $S1P_3$, and $S1P_4$ mRNA levels in the murine spleen 24 h after MCAO. $S1P_2$ remained at undeterminable levels (UD) across all eight biological replicates tested. Fold change (FC) was normalized compared to splenic GAPDH mRNA levels. The Mann–Whitney U-test was applied to calculate statistical differences. Data are presented as median ± IQR; *** $p < 0.001$.

2.6. Recruitment of T_H and T_{REG} Cells to the Peri-Infarct Cortex after Stroke Is Associated with an Altered Cerebral $S1P_R$ Pattern

We wanted to further investigate the previously observed T cell recruitment to the brain (Figure 1E). By qPCR and quantitative immunohistochemistry (IHC), we found that the CL featured unaltered yields of mRNA for CD3 (sham vs. CL; 1.0 ± 0.0 vs. 0.5 ± 0.2, $p = 0.1$, Figure 3A), FoxP3 (sham vs. CL; 1.0 ± 0.0 vs. 0.8 ± 0.6, $p = 0.127$, Figure 3A), and STAT3 (sham vs. CL; 1.0 ± 0.0 vs. 1.9 ± 0.6, $p = 0.2063$, Figure 3A). In contrast, while CD3 and FoxP3 mRNAs were also unaffected in the IL 24 h after MCAO (CD3: sham vs. IL; 1.0 ± 0.0 vs. 2.0 ± 0.7, $p = 0.1$; FoxP3: sham vs. IL; 1.0 ± 0.0 vs. 2.0 ± 1.3, $p = 0.127$, Figure 3A), STAT3 was significantly upregulated compared to sham (sham vs. IL; 1.0 ± 0.0 vs. 2.6 ± 1.3, $p = 0.0079$, Figure 3A). Interestingly, the proclivity for enhanced FoxP3 expression in the IL was close to significance when compared to the CL (CL vs. IL; 0.8 ± 0.6 vs. 2.0 ± 1.3, $p = 0.0625$, Figure 3A).

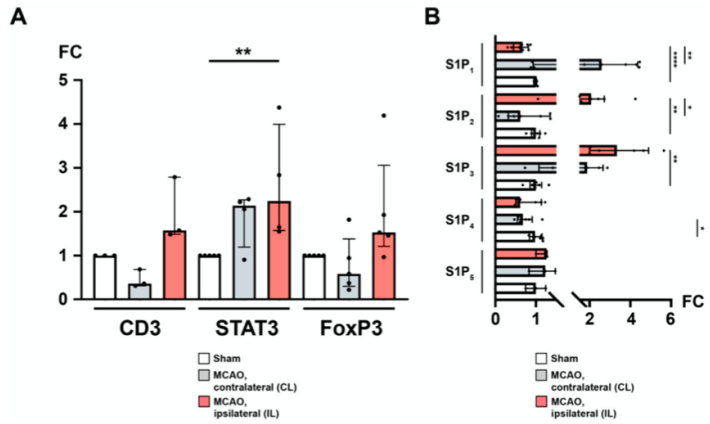

Figure 3. The ipsilateral hemisphere is distinguished by $CD3^+$ $FoxP3^+$ T_H cell recruitment and differential regulation of S1P receptors after acute ischemic stroke. (**A**) mRNA levels of CD3, STAT3, and FoxP3 were quantified by measuring fold change (FC) normalized to GAPDH expression in the murine brain (24 h) after MCAO. An expansion of $CD3^+$ regulatory T_H cells was observed in the ipsilateral hemisphere. (**B**) Likewise, mRNA levels of the sphingosine 1-phosphate receptors $S1P_1$, $S1P_2$, $S1P_3$, $S1P_4$, and $S1P_5$, respectively, were quantified. In particular, $S1P_1$ was subject to a downregulation as opposed to upregulated $S1P_2$ and $S1P_3$ in the ipsilateral hemisphere. The Mann–Whitney U-test was applied to calculate statistical differences between sham (S) and the contralateral hemisphere (CL) or ipsilateral hemisphere (IL) in MCAO-treated mice. A Wilcoxon test was used when comparing CL with IL. In (**A**), each data point refers to the average of four homogenized whole brain lysates (sham), or half-brain lysates, i.e., ipsilateral or contralateral, respectively. The data are presented as median ± IQR; * $p < 0.05$, ** $p < 0.01$, **** $p < 0.0001$.

Previously, sphingosine 1-phosphate receptors were reported to be expressed both on neuronal cells as well as on infiltrating T cells [19,40]. Hence, we were also interested in the differential regulation of sphingosine 1-phosphate receptors in response to focal cerebral ischemia. $S1P_1$ was found to be downregulated in the IL both compared to sham ($S1P_1$: sham vs. IL; 1.0 ± 0.0 vs. 0.6 ± 0.2, $p < 0.0001$, Figure 3B) and to the CL ($S1P_1$: CL vs. IL; 2.7 ± 1.6 vs. 0.6 ± 0.2, $p = 0.0078$) suggesting an S1P-$S1P_1$ ligation with subsequent receptor downregulation. There was no difference between sham and the CL ($S1P_1$: sham vs. CL; 1.0 ± 0.0 vs. 2.7 ± 1.6, $p = 0.2183$, Figure 3B). Regarding $S1P_2$, we could demonstrate a significant upregulation in the IL after MCAO compared to sham ($S1P_2$: sham vs. IL; 1.0 ± 0.1 vs. 2.2 ± 1.1, $p = 0.0022$, Figure 3B) and the CL ($S1P_2$: CL vs. IL; 0.8 ± 0.5 vs. 2.2 ± 1.1, $p = 0.0156$, Figure 3B). There was no difference between sham and the CL ($S1P_2$: sham vs. CL; 1.0 ± 0.1 vs. 0.8 ± 0.5, $p = 0.6126$, Figure 3B). Similarly, $S1P_3$ displayed a profound upregulation in the IL ($S1P_3$: sham vs. IL; 1.0 ± 0.2 vs. 3.5 ± 1.5, $p = 0.0022$, Figure 3B; CL vs. IL; 1.9 ± 0.8 vs. 3.5 ± 1.5, $p = 0.1875$, Figure 3B). The $S1P_3$ expression in the CL was not statistically different from sham ($S1P_3$: sham vs. CL; 1.0 ± 0.2 vs. 1.9 ± 0.8, $p = 0.0823$, Figure 3B). Moreover, $S1P_4$ and $S1P_5$ were also detected in the mouse brain. Compared to sham, neither the CL nor the IL showed any difference after MCAO ($S1P_4$: sham vs. IL; 1.0 ± 0.1 vs. 0.8 ± 0.3, $p = 0.2523$; CL vs. IL; 0.7 ± 0.2 vs. 0.8 ± 0.3, $p = 0.3125$; $S1P_5$: sham vs. CL; 1.0 ± 0.2 vs. 1.2 ± 0.3, $p = 0.7$; sham vs. IL; 1.0 ± 0.2 vs. 1.2 ± 0.2, $p = 0.2$; CL vs. IL; 1.2 ± 0.3 vs. 1.2 ± 0.2, $p > 0.9999$, Figure 3B) except for $S1P_4$, which was downregulated in the CL (sham vs. CL; 1.0 ± 0.1 vs. 0.7 ± 0.2, $p = 0.036$, Figure 3B).

Given the indication for relevant T_H and T_{REG} cell infiltration and a differential expression of $S1P_R$ by qPCR, we sought to confirm these observations using quantitative immunohistochemistry (IHC) for CD3 and FoxP3, respectively.

We detected a significant egress of CD3 T cells from the spleen swiftly after the MCAO intervention had occurred (Figure S3). Our measurements were acquired 3 and 24 h after MCAO, respectively, but some reports do suggest that this process almost coincides with the onset of cerebral ischemia [40]. One day after the intervention, T cells re-appeared both in the white and red pulp, respectively, although at a lower expression level (Figure S3).

Appreciating the reduced T cell frequencies both in the spleen and circulation 24 h after MCAO, we intended to confirm if T cells were recruited towards the brain. For this reason, we defined four regions of interest as potential areas for T cell recruitment: areas equivalent to the peri-infarct cortex, but similarly the white matter area adjacent to the ischemic area from the ipsilateral (IL) and contralateral (CL) hemisphere, respectively (Figure 4A). We found CD3 immunostaining particularly prevalent in the peri-infarct cortex (PIC) (Figure 4(C_4)) and the associated peri-ventricular area (PVA) in the ipsilateral hemisphere (Figure 4(C_3)) in MCAO-operated mice 24 h post-intervention. These changes, to that extent, were not observed neither in the contralateral hemisphere in MCAO mice (Figure 4(C_2,C_1), respectively), nor did any brain area in sham-treated mice express CD3 more abundantly (Figure 4($B_{1–4}$)). These changes in CD3 expression were also quantified (Figure S4).

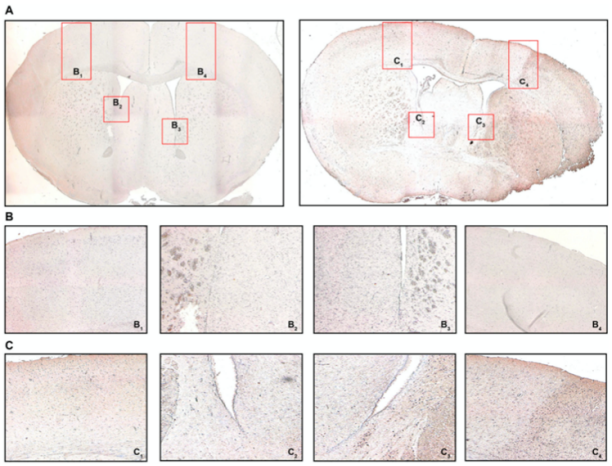

Figure 4. Cerebral recruitment of $CD3^+$ T cells in the peri-infarct cortex and ipsilateral white matter after acute ischemic stroke. (**A**) Coronal brain sections from a sham-operated mouse (left) or a mouse subjected to MCAO (right) 24 h post-intervention. (**B**) B_1 refers to the contralateral cortical area, B_2 refers to the contralateral white matter adjacent to the lateral ventricle, $B_{3/4}$ refer to the ipsilateral equivalents to $B_{1/2}$. (**C**) C_1 refers to the contralateral cortical area, C_2 refers to the contralateral white matter adjacent to the lateral ventricle, $C_{3/4}$ refer to the ipsilateral equivalents to $C_{1/2}$. Positive CD3 immunostaining was characterized by brown-colored cells with condensed nuclei and a subtle surrounding cytoplasmic area pertinent to lymphocytes, particularly in the peri-infarct cortex (C_4) and the ipsilateral white matter (C_3), which was not observed in sham-operated mice (B_3 and B_4, respectively). Original magnifications: (**A**) 2×; (**B**,**C**) 8×.

Using IHC we also found FoxP3 to be expressed by some of the infiltrating cells (Figure 5). Similar to CD3, only the ipsilateral PIC and PVA in MCAO mice did demonstrate relevant FoxP3 immunostaining compared to the CL and sham-operated mice (Figure 5A–C). Quantification revealed very low levels of FoxP3 positivity (Figure S5), aligning well with the literature [41].

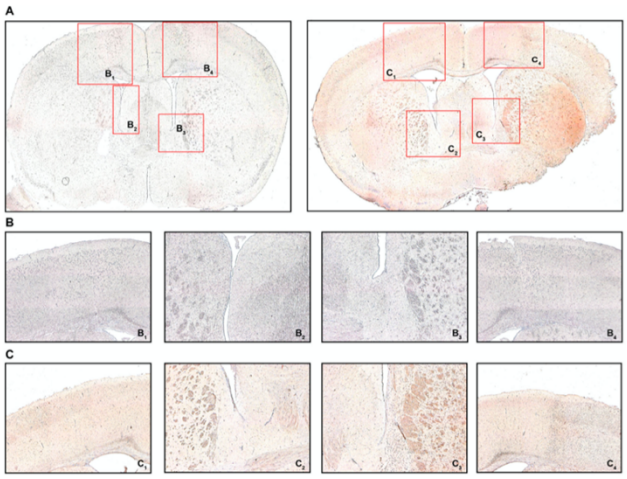

Figure 5. FoxP3 immunohistochemistry (IHC). (**A**) Coronal brain sections from sham-operated mice (left) or MCAO-mice (right) 24 h post-intervention detailing where the respective detailed images were taken from. (**B**) B_1 refers to the contralateral cortical area, B_2 refers to the contralateral white matter adjacent to the lateral ventricle, $B_{3/4}$ refer to the ipsilateral equivalents to $B_{1/2}$. (**C**) C_1 refers to the contralateral cortical area, C_2 refers to the contralateral white matter adjacent to the lateral ventricle, $C_{3/4}$ refer to the ipsilateral equivalents to $C_{1/2}$. Positive FoxP3 immunostaining was characterized by brown-colored cells with condensed nuclei and a subtle surrounding cytoplasmic area pertinent to lymphocytes, particularly in the peri-infarct cortex (C_4) and the ipsilateral white matter (C_3), which was not observed in sham-operated mice (B_3 and B_4, respectively). Original magnifications: (**A**) 2×; (**B**,**C**) 8×.

2.7. Ceramide Species: A Conflicting Chemotactic Agent for Immune Cell Egress?

It has been demonstrated that focal cerebral ischemia leads to a ceramide accumulation in the ischemic cerebral cortex [42]. Therefore, we studied the alterations after murine focal ischemia in the spleen and ischemic cerebral cortex [42]. In the spleen (Figure 6A), sphingosine (Sph), the precursor of S1P, was markedly reduced 24 h after MCAO, although statistic testing was not possible since Sph levels in sham mice were consistently above the upper limit of quantification (ULOQ) (sham vs. MCAO; ULOQ vs. 1644 ± 196.9 pg/mg, Figure 6A). Besides, we could not establish any significant difference in sphinganine (Sgn) levels 24 h after MCAO compared to sham-treated mice (sham vs. MCAO; 473.5 ± 221.7 pg/mg vs. 436.9 ± 78.7 pg/mg, $p > 0.9999$, Figure 6A). C16 concentration in murine spleen showed a striking increase 24 h post-occlusion (sham vs. MCAO; 1506 ± 646.8 pg/mg vs. 3637 ± 361.6 pg/mg, $p = 0.0095$, Figure 6A). Moreover, we demonstrated a significant increase in C18 ceramide levels as well compared to sham-operated mice (sham vs. MCAO; 318.8 ± 54.1 pg/mg vs. 770.2 ± 163.2 pg/mg, $p = 0.004$, Figure 6A). C20 and C24 ceramide levels showed a similar pattern (C20: sham vs. MCAO; 696.6 ± 138.6 pg/mg vs. 1323 ± 293.4 pg/mg, $p = 0.004$; C24: sham vs. MCAO; 2659 ± 843.3 pg/mg vs. 4900 ± 836.1 pg/mg, $p = 0.0081$, Figure 6A).

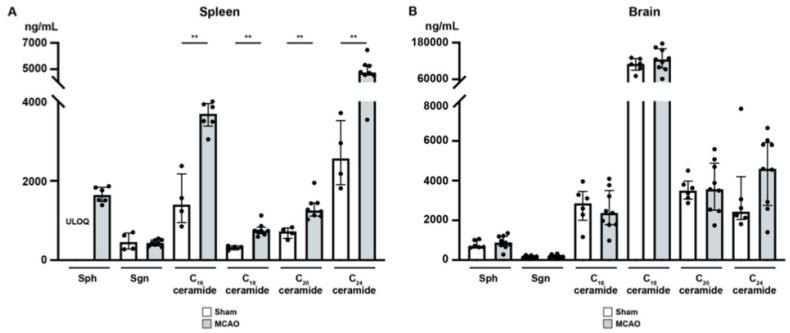

Figure 6. Sphingosine, sphinganine, and ceramide species levels in the spleen and murine brain (24 h) after MCAO acute ischemic stroke. (**A**) Across all the ceramide species tested an increase was seen in the murine spleen (24 h) after MCAO. (**B**) Ceramide species levels in the peri-infarct cortex were unaffected (24 h) after acute ischemic stroke. The Mann–Whitney U-test was applied to calculate statistical differences. The data are presented as median ± IQR; ** $p < 0.01$.

In contrast to the spleen, all ceramide species tested showed no difference in the brain as a consequence of MCAO (Sph: sham vs. MCAO; 788.3 ± 194.1 pg/mg vs. 900.0 ± 331.7 pg/mg, $p = 0.2853$; Sgn: sham vs. MCAO; 170.0 ± 60.7 pg/mg vs. 188.9 ± 74.2 pg/mg, $p = 0.6885$; C16 ceramide: sham vs. MCAO; 2735 ± 964.0 pg/mg vs. 2497 ± 1021 pg/mg, $p = 0.607$; C18 ceramide: sham vs. MCAO; 107.5 ± 21.8 ng/mg vs. 124.8 ± 37.2 ng/mg, $p = 0.4559$; C20 ceramide: sham vs. MCAO; 3553 ± 575.0 pg/mg vs. 3674 ± 1283 pg/mg, $p = 0.8639$; C24 ceramide: sham vs. MCAO; 3248 ± 2184 pg/mg vs. 4483 ± 1808 pg/mg, $p = 0.2721$, Figure 6B).

3. Discussion

This study provides comprehensive data on S1P concentrations in the murine brain, in the circulation, and in secondary lymphoid organs after MCAO and their association with systemic adaptations of the immune system. We found a steep S1P gradient with lowest concentrations in the spleen, moderate concentrations in the circulation, and highest concentrations in the ischemic core 24 h after MCAO. High S1P concentrations in the brain persisted directly in the ischemic lesion 24 h after MCAO with an additional gradient formed between the ischemic core ($S1P^{HIGH}$) and the peri-infarct cortex ($S1P^{LOW}$). We found the S1P gradient to be linked to splenic $S1P_1{}^+$ T cell egress. These evading T cells, being of T_H and T_{REG} cell phenotype, were swiftly recruited towards the brain almost instantly after MCAO. Unaltered ceramide levels but a differential expression of $S1P_R$ were observed in the brain after stroke. We suggest that a differential expression of $S1P_R$ may lure T_H and T_{REG} cells towards an S1P gradient and may be involved with the spatiotemporal positioning of these cells after acute ischemic stroke.

S1P signaling is conceived to be involved in regulating immune responses [26]. Erythrocytes and vascular endothelial cells have been identified as the key determinants of plasma S1P levels [43,44]. The S1P concentration is influenced by the actions of sphingosine kinase 1 (SphK1) and sphingosine kinase 2 (SphK2) [45]. The S1P levels in the blood and lymph are higher compared to tissues [46]. In the circulation, bound to $ApoM^+$-HDL and albumin, S1P reaches high nanomolar concentrations. In contrast, low nanomolar concentrations are observed intracellularly and in interstitial fluids [47]. It was postulated that the chemotactic S1P gradient plays a role in lymphocyte egress directing lymphocytes into the circulation [4,13,48]. Accordingly, disrupting the S1P gradient by 2-acetyl-4-tetrahydroxybutylimidazole, an inhibitor of the S1P lyase, led to lymphopenia and inhibited T cell egress from the thymus, which was mediated by a downregulation of surface $S1P_1$ [49]. Moreover, a deficiency in $S1P_1$ expression was found to impair lymphocyte egress from secondary lymphoid

organs along the S1P gradient [50]. Pharmacological manipulation of $S1P_1$ through fingolimod led to T and B cell sequestration through internalization of $S1P_1$ suggesting the S1P-$S1P_1$ interaction to be the molecular switch of lymphocyte egress [4]. Sustained exposure to S1P downregulates $S1P_1$ resulting in non-responsiveness to S1P-mediated chemotaxis and vice versa [51]. As it appears, the key enzymes SphK1/2 are inversely regulated when $S1P_1$ is ligated by S1P on naïve T cells in the circulation [43]. Furthermore, these lymphocytes failed to egress from the thymus and secondary lymphoid organs [43].

We observed a steep S1P gradient towards the ischemic core after MCAO, whilst S1P was reduced in the peri-infarct cortex. Our findings align well with a study by Hasegawa et al. [19] who demonstrated that $S1P_1$, SphK1, and SphK2 were decreased in the infarct cortex but preserved in the peri-infarct cortex at least 6 h after MCAO. With decreased levels of S1P in the penumbra, the negative feedback loop of S1P ligation to $S1P_1$ is inhibited, resulting in maintained expression of $S1P_1$ and active SphK1/2, respectively [43].

It was shown that NK cell infiltration into the ischemic hemisphere is an extremely swift process happening as early as 3 h post injury [52]. Reports are accumulating that this process applies to adaptive lymphocytes, too. In that respect, various T_H cell populations and T_{REG} cells in the ischemic hemisphere have been found to amass on the first day after MCAO [53–55]. Moreover, it can be argued that neurons are an important source of S1P [56], suggesting that as cerebral blood flow (CBF) decreases and neuronal damage worsens, the release of S1P into the ischemic core could contribute to the maintained high S1P levels [40,57]. This, in turn, would establish a new S1P gradient allowing various immune cell populations to invade the peri-infarct cortex. Our data obtained by qPCR and quantitative immunohistochemistry support the hypothesis of T_H and T_{REG} cell recruitment to the ipsilateral hemisphere after MCAO.

How these cells respond chemotactically to S1P may be subject to their unique $S1P_R$ repertoire [39,58], which we found to be differentially patterned after MCAO. Interestingly, the $S1P_R$ expression pattern was also altered in the contralateral hemisphere after stroke suggesting an additional regulatory function. It has been shown that the $S1P_2$ is more abundantly expressed on vascular endothelial cells after cerebral ischemia [17], involved in vascular permeability and inflammation [59,60] with potential influence on lymphocyte traffic to and within the brain [61]. Moreover, $S1P_2$ was recently linked to a pro-inflammatory response by inducing M1 polarization after cerebral ischemia [62]. In contrast, $S1P_3$ is expressed in embryonic endothelial cells and is required for endothelial cell morphogenesis as well as migration [63–65]. In addition, $S1P_3$ acts as a mediator of P-selectin-mobilizing effects by activating SphK1 [66].

In our study, we report a profound increase in the mRNAs for $S1P_2$ and $S1P_3$ correlating with enhanced CD3 and FoxP3 expression (using qPCR and IHC) 24 h after MCAO predominantly in the ipsilateral hemisphere. Studies have described the unique role of $S1P_3$ in promoting inflammatory responses, mediated through its upregulation in astrocytes [67–69], the activation of RhoA and induction of COX-2, IL-6, and VEGF-α [70]. $S1P_3$ has also been described to recruit macrophages to the site of inflammation [71]. We have found an upregulation of $S1P_3$ in the ischemic brain in accordance with a recent report [40].

In our study, we report higher S1P levels in murine and human plasma compared to secondary lymphoid organs. This may allow lymphocyte egress from the spleen into the circulation. Nevertheless, lymphocytes in the circulation swiftly decreased 3 h after MCAO. In accordance with this finding, previous reports have shown that migration of immune cells is a process which almost coincides with MCAO [53–55]. However, the S1P gradient alone cannot solely account for immune cell migration to the brain as also sham S1P levels in the brain superseded sham S1P levels in the circulation. This suggests that other events such as the presentation of E-selectin by activated endothelium [72], or the expression of L-selectin by activated white blood cells [73,74] may be required for lymphocyte diapedesis in $S1P_2$-loosened endothelial tightness adjacent to the peri-infarct cortex. Additionally, we suggest that the expression of $S1P_{1–5}$ or other glycosphingolipids such as ceramides may foster/mediate immune cell chemotaxis to the brain. In that respect, we report a significant reduction in splenic $S1P_1$ mRNA,

in accordance with an early activation and egress of splenocytes [36]. In this study it was shown that a rapid splenic T cell response was established after the insult had occurred [36]. Moreover, tonsil-resident T cells were reported to be promptly recruited chemotactically into the circulation in response to S1P [48]. However, a contrasting effect was observed towards S1P as soon as these T cells had been recruited into the circulation and this effect was attributed to an altered ratio between $S1P_1$ and $S1P_2$ [48]. We hypothesize that the balanced expression of $S1P_R$ may be subject to change upon activation and recruitment to the effector cell pool.

With regard to ceramides, their complex effects on immune cells have become more and more unraveled. They have been shown to induce apoptosis [75], and to be involved in a re-assembly of the T cell cytoskeleton by intercalating into the plasma membrane due to their lipophilic properties [76]. Here, we showed no significant changes in the level of ceramides in the peri-infarct cortex compared to sham. In contrast, we report increased ceramide levels in the spleen after MCAO, most likely due to the incitement of apoptosis.

Our findings regarding the S1P receptor expression profile after stroke in different compartments indicate an involvement of the systemic and local S1P signaling in immune cell trafficking after stroke. Contributing events, such as inflammation at the stroke site, allowing E-selectin to be expressed by the inflamed endothelium, $S1P_2$ to reduce the extent of tight junctions established by $S1P_1$, and L-selectin expression on activated lymphocytes may all contribute towards T_H and T_{REG} cell rolling and diapedesis through vessels traversing cerebral areas possessing $S1P^{HIGH}$ concentrations.

Taken together, our findings suggest relevant signaling effects triggered by S1P essentially regulating T_H and T_{REG} cell responses, a differential patterning of $S1P_R$ and their swift recruitment towards the injured site and renders ceramides unlikely to regulate lymphocyte recruitment to the brain.

4. Conclusions

We found a steep S1P gradient towards the brain after MCAO in mice and corroborated the clinical significance with a parallel significant increase of plasma S1P after stroke. This was accompanied by a drop of circulating lymphocytes in the context of lower S1P levels in the spleen. Our findings of intricate and organ-specific regulations of the S1P receptor expression profile after acute ischemic stroke suggest systemic and local S1P signaling to be involved in regulating the lymphocyte recruitment towards the peri-infarct region of the brain and systemic stroke-induced immunosuppression. Future studies remain to elucidate the causal effect that $S1P_R$ patterns impose on spatiotemporal positioning and chemotaxis of T_H and T_{REG} cells within the brain. Understanding how these cells can be therapeutically utilized to reduce the detrimental effects caused by ischemic stroke may help to identify pharmacologically exploitable targets for an improved recovery and outcome in patients suffering from ischemic stroke.

5. Materials and Methods

For all experiments, male C57BL/6 mice (strain J, 11–12 weeks, Charles River Laboratories, Sulzfeld, Germany) were used and kept on a 12:12 h light-dark cycle with food and water ad libitum. All animal experiments in this study conformed to the German Protection of Animals Act and the guidelines for care and use of laboratory animals by the local committee (Regierungspräsidium Darmstadt, Germany, FU/1049, 2 April 2015).

5.1. Experimental Model of Middle Cerebral Artery Occlusion

Transient right MCAO was performed for 1 h under anesthesia with 1.5% isoflurane (Abbott, Wiesbaden, Germany) and 0.1 mg/kg buprenorphine (Essex Pharma, Munich, Germany) under spontaneous respiration using a standardized silicon-coated monofilament with a tip diameter of 0.23 mm (Doccol, Redlands, CA, USA). A midline cervical incision was performed, and the right carotid bifurcation was exposed. The monofilament was introduced and advanced along the internal carotid artery occluding the proximal stem of the middle cerebral artery. The reperfusion was initiated by withdrawing the filament after 1 h of focal cerebral ischemia. Following the operation, mice were

monitored until regaining consciousness and returned to their cages. All animals received food and regular drinking water ad libitum. Animals were assessed either 3 or 24 h after reperfusion.

In total, 32 mice were subjected to 1 h of MCAO and harvested 24 h post-intervention, 10 mice were harvested after 3 h whilst, 15 sham-operated mice were harvested after 24 h and employed as controls. Death as a result of the MCAO operation was the sole exclusion criterion in this study. In total, three mice had died (mortality rate: 3/57 = 5.3%) and were therefore excluded from further experimental investigation. All other animals that were subjected to MCAO displayed clear features of ischemia as analyzed by the mNSS score and TTC staining, respectively. The operations were performed unblinded since the operator did not apply any modifications such as drug treatment. However, sample provision for flow cytometry, immunohistochemistry, mass spectrometry, and qPCR assessment were done in a blinded fashion.

5.2. Determination of Sphingolipid Concentrations by High-Performance Liquid Chromatography-Tandem Mass Spectrometry

The quantification of sphingolipids was performed for brain or serum. In total, 10 µL serum was used for lipid analysis. Serum samples were mixed with 190 µL water before the extraction. The samples were mixed with 200 µL extraction buffer (citric acid 30 mM, disodium hydrogen phosphate 40 mM) and 20 µL of the internal standard solution containing sphingosine-d7, sphinganine-d7 (200 ng/mL each), and C18-sphingosine-1-phosphate-d7 (400 ng/mL methanol, all Matreya, State College, PA, USA). The mixture was extracted once with 1000 µL methanol:chloroform:hydrochloric acid (15:83:2, *v/v/v*). The organic phase was evaporated and reconstituted in 100 µL of tetrahydrofuran:water (9:1, *v/v*) containing 0.2% formic acid and 10 mM ammonium formate.

For the determination of the tissue samples, the samples were mixed with 200 µL water and 20 µL internal standard solution and homogenized using a Mixer Mill MM400 (Retsch, Haan, Germany) with five zirconium oxide grinding balls for each sample (25 Hz for 2.5 min). The extraction was processed as described for serum but using 10 µL of the homogenate. For calibration standards and quality control samples preparation, 20 µL of the corresponding working solutions were processed as stated instead of sample.

C20-sphingosine-1-phosphate was determined semiquantitatively by means of a C20-S1P standard. An Agilent 1100 series binary pump (Agilent Technologies, Waldbronn, Germany) equipped with a Luna C8 column (150 × 2 mm ID, 3 µm particle size, 100 Å pore size; Phenomenex, Aschaffenburg, Germany) was used for chromatographic separation under gradient conditions. The HPLC mobile phases consisted of water with 0.2% formic acid and 2 mM ammonium formate (mobile phase A) and acetonitrile:isopropanol:acetone (50:30:20, *v/v/v*) with 0.2% formic acid (mobile phase B). The total running time was 21 min and the injection volume was 15 µL. Acetonitrile with 0.1% formic acid was infused post-column using an isocratic pump at a flow rate of 0.15 mL/min. The MS/MS analyses were performed using a triple quadrupole mass spectrometer API4000 (Sciex, Darmstadt, Germany) equipped with a Turbo V Ion Source operating in positive electrospray ionization Multiple Reaction Monitoring mode.

Data Acquisition was done using Analyst Software V 1.6 and quantification was performed with MultiQuant Software V 3.0 (both Sciex), employing the internal standard method (isotope dilution mass spectrometry).

5.3. Flow Cytometry Analysis of Immune Cells

Brain, blood, and spleen tissues were collected for flow cytometric analyses. Tissue samples were harvested, and single-cell suspensions were obtained. Blood was acquired through cardiac puncture from the right ventricle. Each blood sample, approximately 500 µL blood, was drawn with a syringe filled with heparin solution to prevent clotting and transferred to a Falcon tube with ice-cold 15 mL RPMI-1640 cell culture medium. Falcon tubes were centrifuged (5 min, 1000 rpm, 4 °C) and the supernatant was discarded. Cells were incubated with blocking buffer (100 µL

PBS + 1% FCS + 0.01%NaN_3) and subsequently stained with fluorochrome-conjugated antibodies for 30 min in the dark at 4 °C. Samples were analyzed on a BD FACSCanto II (BD Biosciences, Heidelberg, Germany). The following antibodies were used: CD45-FITC (clone 30F11, Miltenyi Biotec, Bergisch Gladbach, Germany), CD45-PE-Cyanine 7 (Miltenyi Biotec, Bergisch Gladbach, Germany), CD3ε-APC-Vio770 (clone 145-2C11, BD Miltenyi Biotec, Bergisch Gladbach, Germany), CD19-VioBlue (clone 6D5, Miltenyi Biotec, Bergisch Gladbach, Germany), CD11b-APC (clone REA592, Miltenyi Biotec, Bergisch Gladbach, Germany), Ly6G-PE (clone REA526, Miltenyi Biotec, Bergisch Gladbach, Germany), Ly6C-FITC (clone 1G7.G10, Miltenyi Biotec, Bergisch Gladbach, Germany), and $S1P_1$-eFluor660 (clone SW4GYPP, ThermoFisher, Darmstadt, Germany). With respect to the identification of various immune cells in murine compartments cell lineage ontogeny was considered as follows: $CD45^+$ cell (commonly expressed by pan-leukocytes and pan-lymphocytes, i.e., differentiated hematopoietic cells), leukocytes ($CD45^+CD11b^+$), PMN ($CD45^+Ly6G^+$), monocytes ($CD45^+Ly6C^{MODERATE}$), dendritic cells ($CD45^+Ly6C^{HIGH}$), B cells ($CD45^+CD19^+$), T cells ($CD45^+CD3^+$), T_H cells ($CD45^+CD4^+$).

5.4. RNA Isolation, cDNA Synthesis, and Quantitative Real-Time PCR

Total mouse RNA from splenocytes and brain homogenates were extracted using Tri reagent (Sigma-Aldrich T9424, Taufkirchen, Germany) according to the manufacturer's instructions. In brief, the spleen was incised and transferred to an Eppendorf tube containing 1 mL of RPMI medium containing GlutaMAX (Gibco, ThermoFisher Scientific, #61870-010, Darmstadt, Germany). The spleen was dissociated using 70 µM Falcon cell strainer (Corning, #352350) and cells were collected in a 50 mL Falcon tube. The cell suspension was centrifuged (400 rpm, 5 min), followed by red blood cell lysis. Then, 1 mL of Tri reagent was added to the cell pellet and frozen immediately. With respect to the brain, after removal from the skull, the ischemic and contralateral hemispheres were separated and transferred to 15 mL Falcon tubes containing 5 mL of PBS (Gibco, ThermoFisher Scientific, #14287-080, Darmstadt, Germany). Homogenization was achieved using the brain dissociation kit (#130-107-677, Miltenyi Biotec, Bergisch Gladbach, Germany). Again, 1 mL of Tri reagent was added to 100 µL of brain homogenate and RNA was isolated according manufacturer's instructions. The RNA yield was established by NanoDrop (ThermoFisher, Darmstadt, Germany). The A260/A280 ratio at this point was routinely between 1.9 and 2.1. Three technical replicates were used for each condition. A total of 1200 ng of RNA was reverse transcribed into cDNA using the RevertAid First Strand cDNA Synthesis Kit (ThermoFisher Scientific, #K1621, Darmstadt, Germany). Using oligo dT primers, a TaqMan-based real-time PCR quantitation was performed (Applied Biosystems 7500fast, Darmstadt, Germany). Duplex PCR was performed using the following cycling parameters: 95 °C (2 min (only 1st cycle)); 95 °C (5 s) followed by 62 °C (30 s) for 40 cycles. Relative mRNA abundance was calculated using the comparative delta-delta Ct method. The Ct values were normalized by the target mRNA/GAPDH gene average value for all samples. The following TaqMan probes (ThermoFisher Scientific, Darmstadt, Germany) were used: GAPDH (Mm99999915), CD3d (Mm00442746), CD11b [ITGAM] (Mm00434455), IL-6 (Mm00446190), PU.1 [SPI1] (Mm00488140), STAT3 (Mm01219775), FoxP3 (Mm00475162), $S1P_1$ (Mm02619656), $S1P_2$ (PN4441114), $S1P_3$ (Mm02620181), $S1P_4$ (Mm00468695), and $S1P_5$ (Mm02620565).

5.5. Immunohistochemistry

The 3 µm thick paraffin sections were subjected to deparaffinization/hydration as follows: (1) suspension in xylene for 10 min for four times; (2) 5 min in isopropanol twice; (3) 5 min in 96% ethanol twice; (4) 5 min in 70% ethanol; (5) 10 min in double distilled water twice. Antigen unmasking was performed by boiling slides in a citrate-based target retrieval solution (Agilent Dako #S1699, Jena, Germany) for 20 min. Then, the slides were cooled to room temperature and the sections were washed in PBS twice, followed by incubation in 0.1% Triton X-100-PBS for 4 min. The slides were washed with PBS two more times. The slides were blocked for 45 min using an immunoblock solution (Roth #T144.1, Karlsruhe, Germany). The primary antibody against CD3 (clone M-20, Santa Cruz Biotechnology, #sc-1127) or FoxP3 (clone 2A11G9, Santa Cruz Biotechnology, #sc-53876, Dallas, TX, USA) diluted

1:50 in the immunoblock solution was added to the slides and was allowed to incubate for ≥16 h at 4 °C. Signal detection was obtained using Histofine Simple Stain Max PO detection system (#414161F, Nichirei Biosciences Inc., Tokyo, Japan) and DAB peroxidase substrate kit (#SK-4100, Linaris, Vector laboratories, Dossenheim, Germany). Counterstaining was employed using hematoxylin. Finally, images were acquired on a Keyence microscope (BZ-8000K, Osaka, Japan).

5.6. Statistical Analyses

GraphPad Prism 8 (GraphPad Software, LLC, La Jolla, CA, USA) was used for statistical analyses. Results are expressed as median ± interquartile range (IQR) except stated otherwise. Statistical significance was assessed using Wilcoxon test for paired samples and Mann–Whitney or Kruskal–Wallis test for unpaired samples. A p value of <0.05 was considered statistically significant.

Supplementary Materials: The following are available online at http://www.mdpi.com/1422-0067/21/17/6242/s1, Figure S1: Temporal profile of the murine spleen weight after MCAO, Figure S2: Temporal profile of immune cell egress from the murine spleen after MCAO, Figure S3: Splenic CD3+ T cell egress, Figure S4: Quantification of CD3+ T cell recruitment to the brain, Figure S5: Quantification of FoxP3+ TREG cell recruitment to the brain.

Author Contributions: Conceptualization, A.L., R.B., W.P. and R.V.; methodology, A.L., H.K., S.T., N.F., R.B. and R.V.; software, A.L. and J.S.; validation, A.L., J.S., and R.V.; formal analysis, A.L., S.T., R.B. and J.S.; investigation, A.L., H.K., N.F., R.B. and R.V.; resources, J.P., R.B. and W.P.; data curation, A.L.; writing—original draft preparation, A.L. and J.S.; writing—review and editing, A.L., S.T., N.F., H.S., J.P., R.B., W.P., J.S. and R.V.; visualization, A.L. and J.S.; supervision, R.B.; project administration, J.P., R.B. and W.P.; funding acquisition, J.P., R.B. and W.P. All authors have read and agreed to the published version of the manuscript.

Funding: This research was funded by the German Research Foundation (SFB1039/Z1 to N.F.; SFB1039-TPB08 to J.P., R.B. and W.P.), the Leducq Foundation (SphingoNet to J.P. and W.P.), and the Uniscientia Stiftung, Vaduz (to J.P.). J.S. is funded by a scholarship from the German Academic Scholarship Foundation (Studienstiftung des deutschen Volkes). The article processing charges were provided by the Open Access Publication Fund of the Goethe University Frankfurt.

Acknowledgments: The authors would like to acknowledge Niklas Lohfink for his excellent technical assistance throughout the entire study.

Conflicts of Interest: The authors declare no conflict of interest.

Abbreviations

ApoM	Apolipoprotein M
CBF	Cerebral blood flow
CD	Cluster of differentiation molecule
CL	Contralateral
CNS	Central nervous system
COX-2	Cyclooxygenase-2
FC	Fold change
FoxP3	Forkhead box protein P3
GAPDH	Glyceraldehyde-3-phosphate dehydrogenase
IL	Ipsilateral
IL-6	Interleukin-6
IQR	Interquartile range
IR	Ischemia/reperfusion
MCAO	Middle cerebral artery occlusion
mRNA	Messenger ribonucleic acid
PIC	Peri-infarct cortex
PVA	Periventricular area
qPCR	Quantitative real-time polymerase chain reaction
RhoA	Transforming protein RhoA

SCID	Severe combined immunodeficiency
SphK1	Sphingosine kinase 1
SphK2	Sphingosine kinase 2
SPI1	Transcription factor PU.1
STAT3	Signal transducer and activator of transcription 3
S1P	Sphingosine 1-phosphate
$S1P_1$	Sphingosine 1-phosphate receptor 1
$S1P_2$	Sphingosine 1-phosphate receptor 2
$S1P_3$	Sphingosine 1-phosphate receptor 3
$S1P_4$	Sphingosine 1-phosphate receptor 4
$S1P_5$	Sphingosine 1-phosphate receptor 5
S1PR	Sphingosine 1-phophate receptor
VEGF-α	Vascular endothelial growth factor A

References

1. Lippincott-Schwartz, J.; Phair, R.D. Lipids and cholesterol as regulators of traffic in the endomembrane system. *Annu. Rev. Biophys.* **2010**, *39*, 559–5578. [CrossRef] [PubMed]
2. Lingwood, D.; Simons, K. Lipid rafts as a membrane-organizing principle. *Science* **2010**, *327*, 46–50. [CrossRef] [PubMed]
3. Van Brocklyn, J.R.; Jackson, C.A.; Pearl, D.K.; Kotur, M.S.; Snyder, P.J.; Prior, T.W. Sphingosine kinase-1 expression correlates with poor survival of patients with glioblastoma multiforme: Roles of sphingosine kinase isoforms in growth of glioblastoma cell lines. *J. Neuropathol. Exp. Neurol.* **2005**, *64*, 695–705. [CrossRef] [PubMed]
4. Chongsathidkiet, P.; Jackson, C.; Koyama, S.; Loebel, F.; Cui, X.; Farber, S.H.; Woroniecka, K.; Elsamadicy, A.A.; Dechant, C.A.; Kemeny, H.R.; et al. Sequestration of T cells in bone marrow in the setting of glioblastoma and other intracranial tumors. *Nat. Med.* **2018**, *24*, 1459–1468. [CrossRef] [PubMed]
5. Czech, B.; Pfeilschifter, W.; Mazaheri-Omrani, N.; Strobel, M.A.; Kahles, T.; Neumann-Haefelin, T.; Rami, A.; Huwiler, A.; Pfeilschifter, J. The immunomodulatory sphingosine 1-phosphate analog FTY720 reduces lesion size and improves neurological outcome in a mouse model of cerebral ischemia. *Biochem. Biophys. Res. Commun.* **2009**, *389*, 251–256. [CrossRef]
6. Hasegawa, Y.; Suzuki, H.; Sozen, T.; Rolland, W.; Zhang, J.H. Activation of sphingosine 1-phosphate receptor-1 by FTY720 is neuroprotective after ischemic stroke in rats. *Stroke* **2010**, *41*, 368–374. [CrossRef]
7. Lucaciu, A.; Brunkhorst, R.; Pfeilschifter, J.M.; Pfeilschifter, W.; Subburayalu, J. The S1P–S1PR axis in neurological disorders—Insights into current and future therapeutic perspectives. *Cells* **2020**, *9*, 1515. [CrossRef]
8. Brinkmann, V.; Davis, M.D.; Heise, C.E.; Albert, R.; Cottens, S.; Hof, R.; Bruns, C.; Prieschl, E.; Baumruker, T.; Hiestand, P.; et al. The immune modulator FTY720 targets sphingosine 1-phosphate receptors. *J. Biol. Chem.* **2002**, *277*, 21453–21457. [CrossRef]
9. Mandala, S.; Hajdu, R.; Bergstrom, J.; Quackenbush, E.; Xie, J.; Milligan, J.; Thornton, R.; Shei, G.-J.; Card, D.; Keohane, C.; et al. Alteration of lymphocyte trafficking by sphingosine-1-phosphate receptor agonists. *Science* **2002**, *296*, 346–349. [CrossRef]
10. Foster, C.A.; Mechtcheriakova, D.; Storch, M.K.; Balatoni, B.; Howard, L.M.; Bornancin, F.; Wlachos, A.; Sobanov, J.; Kinnunen, A.; Baumruker, T. FTY720 rescue therapy in the dark agouti rat model of experimental autoimmune encephalomyelitis: Expression of central nervous system genes and reversal of blood-brain-barrier damage. *Brain Pathol.* **2009**, *19*, 254–266. [CrossRef]
11. Choi, J.W.; Gardell, S.E.; Herr, D.R.; Rivera, R.; Lee, C.-W.; Noguchi, K.; Teo, S.T.; Yung, Y.C.; Lu, M.; Kennedy, G.; et al. FTY720 (fingolimod) efficacy in an animal model of multiple sclerosis requires astrocyte sphingosine 1-phosphate receptor 1 (S1P1) modulation. *Proc. Natl. Acad. Sci. USA* **2011**, *108*, 751–756. [CrossRef] [PubMed]
12. Eken, A.; Duhen, R.; Singh, A.K.; Fry, M.; Buckner, J.H.; Kita, M.; Bettelli, E.; Oukka, M. S1P1 deletion differentially affects TH17 and regulatory T cells. *Sci. Rep.* **2017**, *7*, 12905. [CrossRef] [PubMed]

13. Matloubian, M.; Lo, C.G.; Cinamon, G.; Lesneski, M.J.; Xu, Y.; Brinkmann, V.; Allende, M.L.; Proia, R.L.; Cyster, J.G. Lymphocyte egress from thymus and peripheral lymphoid organs is dependent on S1P receptor 1. *Nature* **2004**, *427*, 355–360. [CrossRef] [PubMed]
14. Baeyens, A.; Fang, V.; Chen, C.; Schwab, S.R. Exit strategies: S1P signaling and T cell migration. *Trends Immunol.* **2015**, *36*, 778–787. [CrossRef]
15. Chun, J.; Hla, T.; Lynch, K.R.; Spiegel, S.; Moolenaar, W.H. International Union of Basic and Clinical Pharmacology. LXXVIII. Lysophospholipid Receptor Nomenclature. *Pharmacol. Rev.* **2010**, *62*, 579–587. [CrossRef]
16. Cartier, A.; Hla, T. Sphingosine 1-phosphate: Lipid signaling in pathology and therapy. *Science* **2019**, *366*, eaar5551. [CrossRef]
17. Kim, G.S.; Yang, L.; Zhang, G.; Zhao, H.; Selim, M.; McCullough, D.D.; Klug, M.J.; Sanchez, T. Critical role of sphingosine-1-phosphate receptor-2 in the disruption of cerebrovascular integrity in experimental stroke. *Nat. Commun.* **2015**, *6*, 7893. [CrossRef]
18. Pfeilschifter, W.; Czech-Zechmeister, B.; Sujak, M.; Mirceska, A.; Koch, A.; Rami, A.; Steinmetz, H.; Foerch, C.; Huwiler, A.; Pfeilschifter, J. Activation of sphingosine kinase 2 is an endogenous protective mechanism in cerebral ischemia. *Biochem. Biophys. Res. Commun.* **2011**, *413*, 212–217. [CrossRef]
19. Hasegawa, Y.; Suzuki, H.; Altay, O.; Rolland, W.; Zhang, J.H. Role of the sphingosine metabolism pathway on neurons against experimental cerebral ischemia in rats. *Transl. Stroke Res.* **2013**, *4*, 524–532. [CrossRef]
20. Campbell, B.C.V.; De Silva, D.A.; Macleod, M.R.; Coutts, S.B.; Schwamm, L.H.; Davis, S.M.; Donnan, G.A. Ischaemic stroke. *Nat. Rev. Dis. Prim.* **2019**, *5*, 70. [CrossRef]
21. Prabhakaran, S.; Ruff, I.; Bernstein, R.A. Acute stroke intervention: A systematic review. *JAMA* **2015**, *313*, 1451–1462. [CrossRef] [PubMed]
22. Sacchetti, M.L. Is it time to definitely abandon neuroprotection in acute ischemic stroke? *Stroke* **2008**, *39*, 1659–1660. [CrossRef] [PubMed]
23. Brunkhorst, R.; Kanaan, N.; Koch, A.; Ferreirós, N.; Mirceska, A.; Zeiner, P.; Mittelbronn, M.; Derouiche, A.; Steinmetz, H.; Foerch, C.; et al. FTY720 treatment in the convalescence period improves functional recovery and reduces reactive astrogliosis in photothrombotic stroke. *PLoS ONE* **2013**, *8*, e70124. [CrossRef] [PubMed]
24. Nazari, M.; Keshavarz, S.; Rafati, A.; Namavar, M.R.; Haghani, M. Fingolimod (FTY720) improves hippocampal synaptic plasticity and memory deficit in rats following focal cerebral ischemia. *Brain Res. Bull.* **2016**, *124*, 95–102. [CrossRef] [PubMed]
25. Tian, D.-C.; Shi, K.; Zhu, Z.; Yao, J.; Yang, X.; Zhang, S.; Zhang, M.; Gonzales, R.J.; Liu, Q.; Huang, D.; et al. Fingolimod enhances the efficacy of delayed alteplase administration in acute ischemic stroke by promoting anterograde reperfusion and retrograde collateral flow. *Ann. Neurol.* **2018**, *84*, 717–728. [CrossRef] [PubMed]
26. Don-Doncow, N.; Zhang, Y.; Matuskova, H.; Meissner, A. The emerging alliance of sphingosine-1-phosphate signalling and immune cells: From basic mechanisms to implications in hypertension. *Br. J. Pharmacol.* **2019**, *176*, 1989–2001. [CrossRef]
27. Stoll, G.; Jander, S.; Schroeter, M. Inflammation and glial responses in ischemic brain lesions. *Prog. Neurobiol.* **1998**, *56*, 149–171. [CrossRef]
28. Schwab, J.M.; Seid, K.; Schluesener, H.J. Traumatic brain injury induces prolonged accumulation of cyclooxygenase-1 expressing microglia/brain macrophages in rats. *J. Neurotrauma* **2001**, *18*, 881–890. [CrossRef]
29. Iadecola, C.; Anrather, J. The immunology of stroke: From mechanisms to translation. *Nat. Med.* **2011**, *17*, 796–808. [CrossRef]
30. Hurn, P.D.; Subramanian, S.; Parker, S.M.; Afentoulis, M.E.; Kaler, L.J.; Vandenbark, A.A.; Offner, H. T- and B-cell-deficient mice with experimental stroke have reduced lesion size and inflammation. *J. Cereb. Blood Flow Metab.* **2007**, *27*, 1798–1805. [CrossRef]
31. Ajmo, C.T., Jr.; Vernon, D.O.L.; Collier, L.; Hall, A.A.; Garbuzova-Davis, S.; Willing, A.; Pennypacker, K.R. The spleen contributes to stroke-induced neurodegeneration. *J. Neurosci. Res.* **2008**, *86*, 2227–2234. [CrossRef] [PubMed]
32. Offner, H.; Subramanian, S.; Parker, S.M.; Wang, C.; Afentoulis, M.E.; Lewis, A.; Vandenbark, A.A.; Hurn, P.D. Splenic atrophy in experimental stroke is accompanied by increased regulatory T cells and circulating macrophages. *J. Immunol.* **2006**, *176*, 6523–6531. [CrossRef] [PubMed]

33. Gelderblom, M.; Leypoldt, F.; Steinbach, K.; Behrens, D.; Choe, C.-U.; Siler, D.A.; Arumugam, T.V.; Orthey, E.; Gerloff, C.; Tolosa, E.; et al. Temporal and spatial dynamics of cerebral immune cell accumulation in stroke. *Stroke* **2009**, *40*, 1849–1857. [CrossRef] [PubMed]
34. Das, M.; Mohapatra, S.; Mohapatra, S.S. New perspectives on central and peripheral immune responses to acute traumatic brain injury. *J. Neuroinflamm.* **2012**, *9*, 236. [CrossRef]
35. Dirnagl, U.; Iadecola, C.; Moskowitz, M.A. Pathobiology of ischaemic stroke: An integrated view. *Trends Neurosci.* **1999**, *22*, 391–397. [CrossRef]
36. Offner, H.; Vandenbark, A.A.; Hurn, P.D. Effect of experimental stroke on peripheral immunity: CNS ischemia induces profound immunosuppression. *Neuroscience* **2009**, *158*, 1098–1111. [CrossRef]
37. Brinkmann, V.; Cyster, J.G.; Hla, T. FTY720: Sphingosine 1-phosphate receptor-1 in the control of lymphocyte egress and endothelial barrier function. *Am. J. Transplant.* **2004**, *4*, 1019–1025. [CrossRef]
38. Pham, T.H.M.; Okada, T.; Matloubian, M.; Lo, C.G.; Cyster, J.G. S1P1 receptor signaling overrides retention mediated by Gαi-coupled receptors to promote T cell egress. *Immunity* **2008**, *28*, 122–133. [CrossRef]
39. Spiegel, S.; Milstien, S. The outs and the ins of sphingosine-1-phosphate in immunity. *Nat. Rev. Immunol.* **2011**, *11*, 403–415. [CrossRef]
40. Salas-Perdomo, A.; Miró-Mur, F.; Gallizioli, M.; Brait, V.H.; Justicia, C.; Meissner, A.; Urra, X.; Chamorro, A.; Planas, A.M. Role of the S1P pathway and inhibition by fingolimod in preventing hemorrhagic transformation after stroke. *Sci. Rep.* **2019**, *9*, 8309. [CrossRef]
41. Ito, M.; Komai, K.; Mise-Omata, S.; Iizuka-Koga, M.; Noguchi, Y.; Kondo, T.; Sakai, R.; Matsuo, K.; Nakayama, T.; Yoshie, O.; et al. Brain regulatory T cells suppress astrogliosis and potentiate neurological recovery. *Nature* **2019**, *565*, 246–250. [CrossRef] [PubMed]
42. Luger, S.; Schwebler, A.; Vutukuri, R.; Ferreiros Bouzas, M.; Labocha, S.; Schreiber, Y.; Brunkhorst, R.; Steinmetz, H.; Pfeilschifter, J.; Pfeilschifter, W. Beta adrenoceptor blockade ameliorates impaired glucose tolerance and alterations of the cerebral ceramide metabolism in an experimental model of ischemic stroke. *Ther. Adv. Neurol. Disord.* **2018**, *11*. [CrossRef] [PubMed]
43. Pappu, R.; Schwab, S.R.; Cornelissen, I.; Pereira, J.P.; Regard, J.B.; Xu, Y.; Camerer, E.; Zheng, Y.-W.; Huang, Y.; Cyster, J.G.; et al. Promotion of lymphocyte egress into blood and lymph by distinct sources of sphingosine-1-phosphate. *Science* **2007**, *316*, 295–298. [CrossRef] [PubMed]
44. Venkataraman, K.; Lee, Y.-M.; Michaud, J.; Thangada, S.; Ai, Y.; Bonkovsky, H.L.; Parikh, N.S.; Habrukowich, C.; Hla, T. Vascular endothelium as a contributor of plasma sphingosine 1-phosphate. *Circ. Res.* **2008**, *102*, 669–676. [CrossRef] [PubMed]
45. Su, D.; Cheng, Y.; Li, S.; Dai, D.; Zhang, W.; Lv, M. Sphk1 mediates neuroinflammation and neuronal injury via TRAF2/NF-κB pathways in activated microglia in cerebral ischemia reperfusion. *J. Neuroimmunol.* **2017**, *305*, 35–41. [CrossRef] [PubMed]
46. Cyster, J.G.; Schwab, S.R. Sphingosine-1-phosphate and lymphocyte egress from lymphoid organs. *Annu. Rev. Immunol.* **2012**, *30*, 69–94. [CrossRef] [PubMed]
47. Okajima, F. Plasma lipoproteins behave as carriers of extracellular sphingosine 1-phosphate: Is this an atherogenic mediator or an anti-atherogenic mediator? *Biochim. Biophys. Acta* **2002**, *1582*, 132–137. [CrossRef]
48. Drouillard, A.; Neyra, A.; Mathieu, A.-L.; Marçais, A.; Wencker, M.; Marvel, J.; Belot, A.; Walzer, T. Human naive and memory T cells display opposite migratory responses to sphingosine-1 phosphate. *J. Immunol.* **2018**, *200*, 551–557. [CrossRef]
49. Schwab, S.R.; Pereira, J.P.; Matloubian, M.; Xu, Y.; Huang, Y.; Cyster, J.G. Lymphocyte sequestration through S1P lyase inhibition and disruption of S1P gradients. *Science* **2005**, *309*, 1735–1739. [CrossRef]
50. Schwab, S.R.; Cyster, J.G. Finding a way out: Lymphocyte egress from lymphoid organs. *Nat. Immunol.* **2007**, *8*, 1295–1301. [CrossRef]
51. Garris, C.S.; Blaho, V.A.; Hla, T.; Han, M.H. Sphingosine-1-phosphate receptor 1 signalling in T cells: Trafficking and beyond. *Immunology* **2014**, *142*, 347–353. [CrossRef] [PubMed]
52. Gan, Y.; Liu, Q.; Wu, W.; Yin, J.-X.; Bai, X.-F.; Shen, R.; Wang, Y.; Chen, J.; La Cava, A.; Poursine-Laurent, J.; et al. Ischemic neurons recruit natural killer cells that accelerate brain infarction. *Proc. Natl. Acad. Sci. USA* **2014**, *111*, 2704–2709. [CrossRef] [PubMed]
53. Shu, L.; Xu, C.-Q.; Yan, Z.-Y.; Yan, Y.; Jiang, S.-Z.; Wang, Y.-R. Post-stroke microglia induce sirtuin2 expression to suppress the anti-inflammatory function of infiltrating regulatory T cells. *Inflammation* **2019**, *42*, 1968–1979. [CrossRef] [PubMed]

54. Zhou, W.; Liesz, A.; Bauer, H.; Sommer, C.; Lahrmann, B.; Valous, N.; Grabe, N.; Veltkamp, R. Postischemic brain infiltration of leukocyte subpopulations differs among murine permanent and transient focal cerebral ischemia models. *Brain Pathol.* **2013**, *23*, 34–44. [CrossRef]
55. Liesz, A.; Suri-Payer, E.; Veltkamp, C.; Doerr, H.; Sommer, C.; Rivest, S.; Giese, T.; Veltkamp, R. Regulatory T cells are key cerebroprotective immunomodulators in acute experimental stroke. *Nat. Med.* **2009**, *15*, 192–199. [CrossRef]
56. Edsall, L.C.; Spiegel, S. Enzymatic measurement of sphingosine 1-phosphate. *Anal. Biochem.* **1999**, *272*, 80–86. [CrossRef]
57. Chao, H.-C.; Lee, T.-H.; Chiang, C.-S.; Yang, S.-Y.; Kuo, C.-H.; Tang, S.-C. Sphingolipidomics investigation of the temporal dynamics after ischemic brain injury. *J. Proteome Res.* **2019**, *18*, 3470–3478. [CrossRef]
58. Rivera, J.; Proia, R.L.; Olivera, A. The alliance of sphingosine-1-phosphate and its receptors in immunity. *Nat. Rev. Immunol.* **2008**, *8*, 753–763. [CrossRef]
59. Sanchez, T.; Skoura, A.; Wu, M.T.; Casserly, B.; Harrington, E.O.; Hla, T. Induction of vascular permeability by the sphingosine-1-phosphate receptor-2 (S1P2R) and its downstream effectors ROCK and PTEN. *Arterioscler. Thromb. Vasc. Biol.* **2007**, *27*, 1312–1318. [CrossRef]
60. Zhang, G.; Yang, L.; Kim, G.S.; Ryan, K.; Lu, S.; O'Donnell, R.K.; Spokes, K.; Shapiro, N.; Aird, W.C.; Kluk, M.J.; et al. Critical role of sphingosine-1-phosphate receptor 2 (S1PR2) in acute vascular inflammation. *Blood* **2013**, *122*, 443–455. [CrossRef]
61. Kimura, A.; Ohmori, T.; Kashiwakura, Y.; Ohkawa, R.; Madoiwa, S.; Mimuro, J.; Shimazaki, K.; Hoshino, Y.; Yatomi, Y.; Sakata, Y. Antagonism of sphingosine 1-phosphate receptor-2 enhances migration of neural progenitor cells toward an area of brain. *Stroke* **2008**, *39*, 3411–3417. [CrossRef] [PubMed]
62. Sapkota, A.; Gaire, B.P.; Kang, M.-G.; Choi, J.W. S1P2 contributes to microglial activation and M1 polarization following cerebral ischemia through ERK1/2 and JNK. *Sci. Rep.* **2019**, *9*, 12106. [CrossRef] [PubMed]
63. McGiffert, C.; Contos, J.J.A.; Friedman, B.; Chun, J. Embryonic brain expression analysis of lysophospholipid receptor genes suggests roles for $S1P_1$ in neurogenesis and $S1P_3$ in angiogenesis. *FEBS Lett.* **2002**, *531*, 103–108. [CrossRef]
64. Lee, M.J.; Thangada, S.; Claffey, K.P.; Ancellin, N.; Liu, C.H.; Kluk, M.; Volpi, M.; Sha'afi, R.I.; Hla, T. Vascular endothelial cell adherens junction assembly and morphogenesis induced by sphingosine-1-phosphate. *Cell* **1999**, *99*, 301–312. [CrossRef]
65. Paik, J.H.; Ss, C.; Lee, M.J.; Thangada, S.; Hla, T. Sphingosine 1-phosphate-induced endothelial cell migration requires the expression of EDG-1 and EDG-3 receptors and Rho-dependent activation of αvβ3- and β1-containing integrins. *J. Biol. Chem.* **2001**, *276*, 11830–11837. [CrossRef]
66. Nussbaum, C.; Bannenberg, S.; Keul, P.; Gräler, M.H.; Gonçalves-de-Albuquerque, C.F.; Korhonen, H.; von Wnuck Lipinski, K.; Heusch, G.; de Castro Faria Neto, H.C.; Rohwedder, I.; et al. Sphingosine-1-phosphate receptor 3 promotes leukocyte rolling by mobilizing endothelial P-selectin. *Nat. Commun.* **2015**, *6*, 6416. [CrossRef]
67. Hamby, M.E.; Coppola, G.; Ao, Y.; Geschwind, D.H.; Khakh, B.S.; Sofroniew, M.V. Inflammatory mediators alter the astrocyte transcriptome and calcium signaling elicited by multiple G-protein-coupled receptors. *J. Neurosci.* **2012**, *32*, 14489–14510. [CrossRef]
68. Van Doorn, R.; Van Horssen, J.; Verzijl, D.; Witte, M.; Ronken, E.; Van Het Hof, B.; Lakeman, K.; Dijkstra, C.D.; Van Der Valk, P.; Reijerkerk, A.; et al. Sphingosine 1-phosphate receptor 1 and 3 are upregulated in multiple sclerosis lesions. *Glia* **2010**, *58*, 1465–1476. [CrossRef]
69. Wu, Y.-P.; Mizugishi, K.; Bektas, M.; Sandhoff, R.; Proia, R.L. Sphingosine kinase 1/S1P receptor signaling axis controls glial proliferation in mice with Sandhoff disease. *Hum. Mol. Genet.* **2008**, *17*, 2257–2264. [CrossRef]
70. Dusaban, S.S.; Chun, J.; Rosen, H.; Purcell, N.H.; Brown, J.H. Sphingosine 1-phosphate receptor 3 and RhoA signaling mediate inflammatory gene expression in astrocytes. *J. Neuroinflamm.* **2017**, *14*, 111. [CrossRef]
71. Keul, P.; Lucke, S.; von Wnuck Lipinski, K.; Bode, C.; Gräler, M.; Heusch, G.; Levkau, B. Sphingosine-1-phosphate receptor 3 promotes recruitment of monocyte/macrophages in inflammation and atherosclerosis. *Circ. Res.* **2011**, *108*, 314–323. [CrossRef] [PubMed]
72. Huang, J.; Choudhri, T.F.; Winfree, C.J.; McTaggert, R.A.; Kiss, S.; Mocco, J.; Kim, L.J.; Protopsaltis, T.S.; Zhang, Y.; Pinsky, D.J.; et al. Postischemic cerebrovascular E-selectin expression mediates tissue injury in murine stroke. *Stroke* **2000**, *31*, 3047–3053. [CrossRef] [PubMed]

73. Ruehl, M.L.; Orozco, J.A.; Stoker, M.B.; McDonagh, P.F.; Coull, B.M.; Ritter, L.S. Protective effects of inhibiting both blood and vascular selectins after stroke and reperfusion. *Neurol. Res.* **2002**, *24*, 226–232. [CrossRef]
74. Yilmaz, G.; Granger, D.N. Cell adhesion molecules and ischemic stroke. *Neurol. Res.* **2008**, *30*, 783–793. [CrossRef]
75. Maceyka, M.; Spiegel, S. Sphingolipid metabolites in inflammatory disease. *Nature* **2014**, *510*, 58–67. [CrossRef]
76. Gassert, E.; Avota, E.; Harms, H.; Krohne, G.; Gulbins, E.; Schneider-Schaulies, S. Induction of membrane ceramides: A novel strategy to interfere with T lymphocyte cytoskeletal reorganisation in viral immunosuppression. *PLoS Pathog.* **2009**, *5*, e1000623. [CrossRef]

7. Darstellung des eigenen Anteils an der Publikation

Die in der Publikation veröffentlichten Ergebnisse beruhen auf den Daten meines Dissertationsprojektes und der Artikel wurde federführend von mir entworfen und anhand der Reviewervorgaben angepasst.

8. Literaturverzeichnis:

1. Campbell BCV, De Silva DA, Macleod MR, et al. Ischaemic stroke. *Nat Rev Dis Prim*. 2019;5(1):70. doi:10.1038/s41572-019-0118-8
2. Johnson CO, Nguyen M, Roth GA, et al. Global, regional, and national burden of stroke, 1990–2016: a systematic analysis for the Global Burden of Disease Study 2016. *Lancet Neurol*. 2019;18(5):439-458. doi:10.1016/S1474-4422(19)30034-1
3. Gomez CR. Editorial: Time is brain! *J Stroke Cerebrovasc Dis*. 1993;3(1):1-2. doi:10.1016/S1052-3057(10)80125-9
4. Saver JL. Time is brain - Quantified. *Stroke*. 2006;37(1):263-266. doi:10.1161/01.STR.0000196957.55928.ab
5. Berkhemer OA, Fransen PSS, Beumer D, et al. A Randomized Trial of Intraarterial Treatment for Acute Ischemic Stroke. *N Engl J Med*. 2015;372(1):11-20. doi:10.1056/NEJMoa1411587
6. Goyal M, Demchuk AM, Menon BK, et al. Randomized assessment of rapid endovascular treatment of ischemic stroke. *N Engl J Med*. 2015;372(11):1019-1030. doi:10.1056/NEJMoa1414905
7. Campbell BCV, Mitchell PJ, Kleinig TJ, et al. Endovascular therapy for ischemic stroke with perfusion-imaging selection. *N Engl J Med*. 2015;372(11):1009-1018. doi:10.1056/NEJMoa1414792
8. Jovin TG, Chamorro A, Cobo E, et al. Thrombectomy within 8 hours after symptom onset in ischemic stroke. *N Engl J Med*. 2015;372(24):2296-2306. doi:10.1056/NEJMoa1503780
9. Saver JL, Goyal M, Bonafe A, et al. Stent-retriever thrombectomy after intravenous t-PA vs. t-PA alone in stroke. *N Engl J Med*. 2015;372(24):2285-2295. doi:10.1056/NEJMoa1415061
10. Bracard S, Ducrocq X, Mas JL, et al. Mechanical thrombectomy after intravenous alteplase versus alteplase alone after stroke (THRACE): a randomised controlled trial. *Lancet Neurol*. 2016;15(11):1138-1147. doi:10.1016/S1474-4422(16)30177-6
11. Mistry EA, Mistry AM, Nakawah MO, et al. Mechanical Thrombectomy Outcomes with and Without Intravenous Thrombolysis in Stroke Patients: A Meta-Analysis. *Stroke*. 2017;48(9):2450-2456. doi:10.1161/STROKEAHA.117.017320
12. Minnerup J, Wersching H, Teuber A, et al. Outcome After Thrombectomy and Intravenous Thrombolysis in Patients With Acute Ischemic Stroke. *Stroke*. 2016;47(6):1584-1592. doi:10.1161/STROKEAHA.116.012619
13. Yaghi S, Eisenberger A, Willey JZ. Symptomatic Intracerebral Hemorrhage in Acute Ischemic Stroke After Thrombolysis With Intravenous Recombinant Tissue Plasminogen Activator: A Review of Natural History and Treatment. *JAMA Neurol*. 2014;71(9):1181. doi:10.1001/JAMANEUROL.2014.1210
14. Anrather J, Iadecola C. Inflammation and Stroke: An Overview. *Neurotherapeutics*. 2016;13(4):661. doi:10.1007/S13311-016-0483-X
15. Yaghi S, Willey JZ, Cucchiara B, et al. Treatment and Outcome of Hemorrhagic Transformation After Intravenous Alteplase in Acute Ischemic Stroke: A Scientific Statement for Healthcare Professionals From the American Heart Association/American Stroke Association. *Stroke*. 2017;48(12):e343-e361. doi:10.1161/STR.0000000000000152
16. Ma G, Pan Z, Kong L, Du G. Neuroinflammation in hemorrhagic transformation after tissue plasminogen activator thrombolysis: Potential mechanisms, targets, therapeutic drugs and biomarkers. *Int Immunopharmacol*. 2021;90:107216. doi:10.1016/J.INTIMP.2020.107216
17. Jickling GC, Liu D, Stamova B, et al. Hemorrhagic transformation after ischemic stroke in animals and humans. *J Cereb Blood Flow Metab*. 2014;34(2):185-199. doi:10.1038/jcbfm.2013.203
18. Maros ME, Brekenfeld C, Broocks G, et al. Number of Retrieval Attempts Rather Than Procedure Time Is Associated With Risk of Symptomatic Intracranial Hemorrhage. *Stroke*. 2021;52(5):1580-1588. doi:10.1161/STROKEAHA.120.031242
19. Hill MD, Goyal M, Menon BK, et al. Efficacy and safety of nerinetide for the treatment of acute ischaemic stroke (ESCAPE-NA1): a multicentre, double-blind, randomised controlled trial. *Lancet*. 2020;395(10227):878-887. doi:10.1016/S0140-6736(20)30258-0
20. Iadecola C, Anrather J. The immunology of stroke: From mechanisms to translation. *Nat Med*. 2011;17(7):796-808. doi:10.1038/nm.2399
21. Weimar C, Ziegler A, König IR, Diener HC. Predicting functional outcome and survival after acute ischemic stroke. *J Neurol*. 2002;249(7):888-895. doi:10.1007/s00415-002-0755-8
22. Paciaroni M, Agnelli G, Corea F, et al. Early hemorrhagic transformation of brain infarction: Rate, predictive factors, and influence on clinical outcome: Results of a prospective multicenter study. *Stroke*. 2008;39(8):2249-2256. doi:10.1161/STROKEAHA.107.510321
23. Larrue V, Kummer R von, Müller A, Bluhmki E. Risk Factors for Severe Hemorrhagic Transformation in Ischemic Stroke Patients Treated With Recombinant Tissue Plasminogen Activator. *Stroke*. 2001;32(2):438-441. doi:10.1161/01.STR.32.2.438
24. Lees KR, Bluhmki E, von Kummer R, et al. Time to treatment with intravenous alteplase and outcome in stroke: an updated pooled analysis of ECASS, ATLANTIS, NINDS, and EPITHET trials.

Lancet. 2010;375(9727):1695-1703. doi:10.1016/S0140-6736(10)60491-6
25. Yang P, Zhang Y, Zhang L, et al. Endovascular Thrombectomy with or without Intravenous Alteplase in Acute Stroke. *https://doi.org/101056/NEJMoa2001123*. 2020;382(21):1981-1993. doi:10.1056/NEJMOA2001123
26. Montaner J, Molina CA, Monasterio J, et al. Matrix Metalloproteinase-9 Pretreatment Level Predicts Intracranial Hemorrhagic Complications After Thrombolysis in Human Stroke. *Circulation*. 2003;107(4):598-603. doi:10.1161/01.CIR.0000046451.38849.90
27. Gasche Y, Copin C, Sugawara T, et al. Matrix Metalloproteinase Inhibition Prevents Oxidative Stress-Associated Blood-Brain Barrier Disruption After Transient Focal Cerebral Ischemia. *J Cereb Blood Flow Metab*. 2001;21(12):1393-1400. doi:10.1097/00004647-200112000-00003
28. Heo HJ, Lucero J, Abumiya T, et al. Matrix Metalloproteinases Increase Very Early During Experimental Focal Cerebral Ischemia. *J Cereb Blood Flow Metab*. 1999;19(6):624-633. doi:10.1097/00004647-199906000-00005
29. Wang X, Tsuji K, Lee SR, et al. Mechanisms of hemorrhagic transformation after tissue plasminogen activator reperfusion therapy for ischemic stroke. *Stroke*. 2004;35(11 Suppl 1):2726-2730. doi:10.1161/01.STR.0000143219.16695.af
30. Krueger M, Bechmann I, Immig K, et al. Blood-brain barrier breakdown involves four distinct stages of vascular damage in various models of experimental focal cerebral ischemia. *J Cereb Blood Flow Metab*. 2015;35(2):292-303. doi:10.1038/jcbfm.2014.199
31. Strbian D, Durukan A, Pitkonen M, et al. The blood-brain barrier is continuously open for several weeks following transient focal cerebral ischemia. *Neuroscience*. 2008;153(1):175-181. doi:10.1016/j.neuroscience.2008.02.012
32. Kassner A, Merali Z. Assessment of Blood–Brain Barrier Disruption in Stroke. *Stroke*. 2015;46(11):3310-3315. doi:10.1161/STROKEAHA.115.008861
33. Paciaroni M, Agnelli G, Micheli S, Caso V. Efficacy and safety of anticoagulant treatment in acute cardioembolic stroke: A meta-analysis of randomized controlled trials. *Stroke*. 2007;38(2):423-430. doi:10.1161/01.STR.0000254600.92975.1F
34. Álvarez-Sabín J, Maisterra O, Santamarina E, Kase CS. Factors influencing haemorrhagic transformation in ischaemic stroke. *Lancet Neurol*. 2013;12(7):689-705. doi:10.1016/S1474-4422(13)70055-3
35. Pfeilschifter W, Spitzer D, Czech-Zechmeister B, et al. Increased risk of hemorrhagic transformation in ischemic stroke occurring during warfarin anticoagulation: An experimental study in mice. *Stroke*. 2011;42(4):1116-1121. doi:10.1161/STROKEAHA.110.604652
36. Meinel TR, Kniepert JU, Seiffge DJ, et al. Endovascular stroke treatment and risk of intracranial hemorrhage in anticoagulated patients. *Stroke*. 2020;51(3):892-898. doi:10.1161/STROKEAHA.119.026606
37. Harenberg J, Schreiner R, Hetjens S, Weiss C. Detecting Anti-IIa and Anti-Xa Direct Oral Anticoagulant (DOAC) Agents in Urine using a DOAC Dipstick. *Semin Thromb Hemost*. 2019;45(3):275-284. doi:10.1055/s-0038-1668098
38. Purrucker JC, Haas K, Wolf M, et al. Haemorrhagic Transformation after Ischaemic Stroke in Patients Taking Non-vitamin K Antagonist Oral Anticoagulants. *J Stroke*. 2017;19(1):67. doi:10.5853/JOS.2016.00542
39. Lucaciu A, Brunkhorst R, Pfeilschifter JM, et al. The S1P-S1PR Axis in Neurological Disorders-Insights into Current and Future Therapeutic Perspectives. *Cells*. 2020;9(6). doi:10.3390/cells9061515
40. Gaire BP, Lee CH, Sapkota A, et al. Identification of Sphingosine 1-Phosphate Receptor Subtype 1 (S1P1) as a Pathogenic Factor in Transient Focal Cerebral Ischemia. *Mol Neurobiol*. 2018;55(3):2320-2332. doi:10.1007/s12035-017-0468-8
41. LaMontagne K, Littiewood-Evans A, Schnell C, et al. Antagonism of sphingosine-1-phosphate receptors by FTY720 inhibits angiogenesis and tumor vascularization. *Cancer Res*. 2006;66(1):221-231. doi:10.1158/0008-5472.CAN-05-2001
42. Quancard J, Bollbuck B, Janser P, et al. A potent and selective S1P1 antagonist with efficacy in experimental autoimmune encephalomyelitis. *Chem Biol*. 2012;19(9):1142-1151. doi:10.1016/j.chembiol.2012.07.016
43. Thangada S, Khanna KM, Blaho VA, et al. Cell-surface residence of sphingosine 1-phosphate receptor 1 on lymphocytes determines lymphocyte egress kinetics. *J Exp Med*. 2010;207(7):1475-1483. doi:10.1084/jem.20091343
44. Brinkmann V, Pinschewer D, Feng L, Chen S. FTY720: altered lymphocyte traffic results in allograft protection. *Transplantation*. 2001;72(5):764-769. doi:10.1097/00007890-200109150-00002
45. Kim Y-M, Sachs T, Asavaroengchai W, et al. Graft-versus-host disease can be separated from graft-versus-lymphoma effects by control of lymphocyte trafficking with FTY720. *J Clin Invest*. 2003;111(5):659. doi:10.1172/JCI16950
46. Brinkmann V, Billich A, Baumruker T, et al. Fingolimod (FTY720): Discovery and development of an oral drug to treat multiple sclerosis. *Nat Rev Drug Discov*. 2010;9(11):883-897. doi:10.1038/nrd3248
47. Czech B, Pfeilschifter W, Mazaheri-Omrani N, et al. The immunomodulatory sphingosine 1-phosphate analog FTY720 reduces lesion size and improves neurological outcome in a mouse model of cerebral ischemia. *Biochem Biophys Res Commun*. 2009;389(2):251-256.

doi:10.1016/j.bbrc.2009.08.142
48. Kraft P, Göb E, Schuhmann MK, et al. FTY720 ameliorates acute ischemic stroke in mice by reducing thrombo-infammation but not by direct neuroprotection. *Stroke*. 2013;44(11):3202-3210. doi:10.1161/STROKEAHA.113.002880
49. Pfeilschifter W, Czech-Zechmeister B, Sujak M, et al. Activation of sphingosine kinase 2 is an endogenous protective mechanism in cerebral ischemia. *Biochem Biophys Res Commun*. 2011;413(2):212-217. doi:10.1016/j.bbrc.2011.08.070
50. Hannun YA, Obeid LM. Principles of bioactive lipid signalling: Lessons from sphingolipids. *Nat Rev Mol Cell Biol*. 2008;9(2):139-150. doi:10.1038/nrm2329
51. Obeid L, Linardic C, Karolak L, Hannun Y. Programmed cell death induced by ceramide. *Science (80-)*. 1993;259(5102):1769-1771. doi:10.1126/SCIENCE.8456305
52. Venable ME, Lee JY, Smyth MJ, Bielawska A, Obeid LM. Role of Ceramide in Cellular Senescence. *J Biol Chem*. 1995;270(51):30701-30708. doi:10.1074/JBC.270.51.30701
53. Herr I, Martin-Villalba A, Kurz E, et al. FK506 prevents stroke-induced generation of ceramide and apoptosis signaling. *Brain Res*. 1999;826(2):210-219. doi:10.1016/S0006-8993(99)01288-3
54. Kubota M, Narita K, Nakagomi T, et al. Sphingomyelin changes in rat cerebral cortex during focal ischemia. *Neurol Res*. 1996;18(4):337-341. doi:10.1080/01616412.1996.11740432
55. Nakane M, Kubota M, Nakagomi T, et al. Lethal forebrain ischemia stimulates sphingomyelin hydrolysis and ceramide generation in the gerbil hippocampus. *Neurosci Lett*. 2000;296(2-3):89-92. doi:10.1016/S0304-3940(00)01655-4
56. Ohtani R, Tomimoto H, Kondo T, et al. Upregulation of ceramide and its regulating mechanism in a rat model of chronic cerebral ischemia. *Brain Res*. 2004;1023(1):31-40. doi:10.1016/j.brainres.2004.07.024
57. Yu ZF, Nikolova-Karakashian M, Zhou D, Cheng G, Schuchman EH, Mattson MP. Pivotal role for acidic sphingomyelinase in cerebral ischemia-induced ceramide and cytokine production, and neuronal apoptosis. *J Mol Neurosci*. 2000;15(2):85-97. doi:10.1385/JMN:15:2:85
58. Novgorodov SA, Gudz TI. Ceramide and mitochondria in ischemic brain injury. *Int J Biochem Mol Biol*. 2011;2(4):347-61. Epub 2011 Nov 25. PMID:22187669; PMCID: PMC3242427.
59. Novgorodov SA, Gudz TI. Ceramide and mitochondria in ischemia/reperfusion. *J Cardiovasc Pharmacol*. 2009;53(3):198-208. doi:10.1097/FJC.0b013e31819b52d5
60. De Wit NM, Den Hoedt S, Martinez-Martinez P, et al. Astrocytic ceramide as possible indicator of neuroinflammation. *J Neuroinflammation*. 2019 Feb;16(1):48. doi:10.1186/s12974-019-1436-1
61. Obinata H, Hla T. Sphingosine 1-phosphate and inflammation. *Int Immunol*. 2019;31(9):617-625. doi:10.1093/intimm/dxz037
62. Bode C, Sensken S-C, Peest U, et al. Erythrocytes serve as a reservoir for cellular and extracellular sphingosine 1-phosphate. *J Cell Biochem*. 2010;109(6):1232-1243. doi:10.1002/JCB.22507
63. Pham THM, Baluk P, Xu Y, et al. Lymphatic endothelial cell sphingosine kinase activity is required for lymphocyte egress and lymphatic patterning. *J Exp Med*. 2010;207(1):17. doi:10.1084/JEM.20091619
64. Tani M, Sano T, Ito M, Igarashi Y. Mechanisms of sphingosine and sphingosine 1-phosphate generation in human platelets. *J Lipid Res*. 2005;46(11):2458-2467. doi:10.1194/JLR.M500268-JLR200
65. Pappu R, Schwab SR, Cornelissen I, et al. Promotion of lymphocyte egress into blood and lymph by distinct sources of sphingosine-1-phosphate. *Science*. 2007;316(5822):295-298. doi:10.1126/science.1139221
66. Takabe K, Paugh SW, Milstien S, Spiegel S. "Inside-Out" Signaling of Sphingosine-1-Phosphate: Therapeutic Targets. *Pharmacol Rev*. 2008;60(2):181-195. doi:10.1124/PR.107.07113
67. Kim GS, Yang L, Zhang G, et al. Critical role of sphingosine-1-phosphate receptor-2 in the disruption of cerebrovascular integrity in experimental stroke. *Nat Commun*. 2015;6:7893. doi:10.1038/ncomms8893
68. Campos F, Qin T, Castillo J, et al. Fingolimod reduces hemorrhagic transformation associated with delayed tissue plasminogen activator treatment in a mouse thromboembolic model. *Stroke*. 2013;44(2):505-511. doi:10.1161/STROKEAHA.112.679043
69. Salas-Perdomo A, Miró-Mur F, Gallizioli M, et al. Role of the S1P pathway and inhibition by fingolimod in preventing hemorrhagic transformation after stroke. *Sci Rep*. 2019;9(1):8309. doi:10.1038/s41598-019-44845-5
70. Sun N, Keep RF, Hua Y, Xi G. Critical Role of the Sphingolipid Pathway in Stroke: a Review of Current Utility and Potential Therapeutic Targets. *Transl Stroke Res*. 2016;7(5):420-438. doi:10.1007/s12975-016-0477-3
71. Don-Doncow N, Zhang Y, Matuskova H, Meissner A. The emerging alliance of sphingosine-1-phosphate signalling and immune cells: from basic mechanisms to implications in hypertension. *Br J Pharmacol*. 2019;176(12):1989-2001. doi:10.1111/bph.14381
72. Su D, Cheng Y, Li S, Dai D, Zhang W, Lv M. Sphk1 mediates neuroinflammation and neuronal injury via TRAF2/NF-κB pathways in activated microglia in cerebral ischemia reperfusion. *J Neuroimmunol*. 2017;305:35-41. doi:10.1016/j.jneuroim.2017.01.015
73. Chongsathidkiet P, Jackson C, Koyama S, et al. Sequestration of T cells in bone marrow in the setting of glioblastoma and other intracranial tumors. *Nat Med*. 2018;24(9):1459-1468.

doi:10.1038/s41591-018-0135-2
74. Matloubian M, Lo CG, Cinamon G, et al. Lymphocyte egress from thymus and peripheral lymphoid organs is dependent on S1P receptor 1. *Nature*. 2004;427(6972):355-360. doi:10.1038/nature02284
75. Huwiler A, Zangemeister-Wittke U. The sphingosine 1-phosphate receptor modulator fingolimod as a therapeutic agent: Recent findings and new perspectives. *Pharmacol Ther*. 2018;185:34-49. doi:10.1016/j.pharmthera.2017.11.001
76. Hasegawa Y, Suzuki H, Altay O, Rolland W, Zhang JH. Role of the Sphingosine Metabolism Pathway on Neurons Against Experimental Cerebral Ischemia in Rats. *Transl Stroke Res*. 2013;4(5):524-532. doi:10.1007/s12975-013-0260-7
77. Rivera J, Proia RL, Olivera A. The alliance of sphingosine-1-phosphate and its receptors in immunity. *Nat Rev Immunol*. 2008;8(10):753-763. doi:10.1038/nri2400
78. Shu L, Xu C-Q, Yan Z-Y, Yan Y, Jiang S-Z, Wang Y-R. Post-Stroke Microglia Induce Sirtuin2 Expression to Suppress the Anti-inflammatory Function of Infiltrating Regulatory T Cells. *Inflammation*. 2019;42(6):1968-1979. doi:10.1007/s10753-019-01057-3
79. Zhou W, Liesz A, Bauer H, et al. Postischemic brain infiltration of leukocyte subpopulations differs among murine permanent and transient focal cerebral ischemia models. *Brain Pathol*. 2013;23(1):34-44. doi:10.1111/j.1750-3639.2012.00614.x
80. Liesz A, Suri-Payer E, Veltkamp C, et al. Regulatory T cells are key cerebroprotective immunomodulators in acute experimental stroke. *Nat Med*. 2009;15(2):192-199. doi:10.1038/nm.1927
81. Edsall LC, Spiegel S. Enzymatic measurement of sphingosine 1-phosphate. *Anal Biochem*. 1999;272(1):80-86. doi:10.1006/abio.1999.4157
82. Spiegel S, Milstien S. The outs and the ins of sphingosine-1-phosphate in immunity. *Nat Rev Immunol*. 2011;11(6):403-415. doi:10.1038/nri2974
83. Kimura A, Ohmori T, Kashiwakura Y, et al. Antagonism of sphingosine 1-phosphate receptor-2 enhances migration of neural progenitor cells toward an area of brain. *Stroke*. 2008;39(12):3411-3417. doi:10.1161/STROKEAHA.108.514612
84. McGiffert C, Contos JJ., Friedman B, Chun J. Embryonic brain expression analysis of lysophospholipid receptor genes suggests roles for *s1p* $_{1}$ in neurogenesis and *s1p* $_{1\text{-}3}$ in angiogenesis. *FEBS Lett*. 2002;531(1):103-108. doi:10.1016/S0014-5793(02)03404-X
85. Lee MJ, Thangada S, Claffey KP, et al. Vascular endothelial cell adherens junction assembly and morphogenesis induced by sphingosine-1-phosphate. *Cell*. 1999;99(3):301-312. doi:10.1016/s0092-8674(00)81661-x
86. Paik JH, Chae SS, Lee MJ, Thangada S, Hla T. Sphingosine 1-Phosphate-induced Endothelial Cell Migration Requires the Expression of EDG-1 and EDG-3 Receptors and Rho-dependent Activation of αvβ3- and β1-containing Integrins. *J Biol Chem*. 2001;276(15):11830-11837. doi:10.1074/jbc.M009422200
87. Sanchez T, Skoura A, Wu MT, Casserly B, Harrington EO, Hla T. Induction of vascular permeability by the sphingosine-1-phosphate receptor-2 (S1P2R) and its downstream effectors ROCK and PTEN. *Arterioscler Thromb Vasc Biol*. 2007;27(6):1312-1318. doi:10.1161/ATVBAHA.107.143735
88. Zhang G, Yang L, Kim GS, et al. Critical role of sphingosine-1-phosphate receptor 2 (S1PR2) in acute vascular inflammation. *Blood*. 2013;122(3):443-455. doi:10.1182/blood-2012-11-467191
89. Nussbaum C, Bannenberg S, Keul P, et al. Sphingosine-1-phosphate receptor 3 promotes leukocyte rolling by mobilizing endothelial P-selectin. *Nat Commun*. 2015;6(1):1-12. doi:10.1038/ncomms7416
90. Gaire BP, Song M-R, Choi JW. Sphingosine 1-phosphate receptor subtype 3 (S1P3) contributes to brain injury after transient focal cerebral ischemia via modulating microglial activation and their M1 polarization. *J Neuroinflammation*. 2018;15(1):284. doi:10.1186/s12974-018-1323-1
91. Malone K, Diaz ACD, Shearer JA, Moore AC, Waeber C. The effect of fingolimod on regulatory T cells in a mouse model of brain ischaemia. *J Neuroinflammation*. 2021;18(1). doi:10.1186/S12974-021-02083-5
92. Cramer J V., Benakis C, Liesz A. T cells in the post-ischemic brain: Troopers or paramedics? *J Neuroimmunol*. 2019;326:33-37. doi:10.1016/J.JNEUROIM.2018.11.006
93. Ito M, Komai K, Mise-Omata S, et al. Brain regulatory T cells suppress astrogliosis and potentiate neurological recovery. *Nature*. 2019;565(7738):246-250. doi:10.1038/s41586-018-0824-5

9. Anhang mit Originaldaten

Article

A Sphingosine 1-Phosphate Gradient is Linked to the Cerebral Recruitment of T Helper and Regulatory T Helper Cells during Acute Ischemic Stroke

Alexandra Lucaciu [1,*], Hannah Kuhn [1], Sandra Trautmann [2], Nerea Ferreirós [2], Helmuth Steinmetz [1], Josef Pfeilschifter [3], Robert Brunkhorst [1,4], Waltraud Pfeilschifter [1], Julien Subburayalu [5,†] and Rajkumar Vutukuri [3,*,†]

[1] Department of Neurology, Goethe University Frankfurt, 60528 Frankfurt am Main, Germany; alexandra.lucaciu@kgu.de (A.L.); hannah.kuhn@gmail.com (H.K.); h.steinmetz@em.uni-frankfurt.de (H.S.); rbrunkhorst@ukaachen.de (R.B.); waltraud.pfeilschifter@kgu.de (W.P.)
[2] Institute of Clinical Pharmacology, Pharmazentrum Frankfurt, Goethe University Frankfurt, 60528 Frankfurt am Main, Germany; trautmann@med.uni-frankfurt.de (S.T.); ferreirosbouzas@em.uni-frankfurt.de (N.F.)
[3] Institute of General Pharmacology and Toxicology, Pharmazentrum Frankfurt, Goethe University Frankfurt, 60528 Frankfurt am Main, Germany; pfeilschifter@em.uni-frankfurt.de (J.P.); vutukuri@med.uni-frankfurt.de (R.V.)
[4] Department of Neurology, RWTH Aachen University, 52074 Aachen, Germany
[5] Department of Medicine, University of Cambridge, Cambridge CB2 0QQ, UK; js2380@cam.ac.uk (J.S.)
* Correspondence: alexandra.lucaciu@kgu.de (A.L.); vutukuri@med.uni-frankfurt.de (R.V.)
† These authors contributed equally.

Received: 07 July 2020; Revised: 12 August 2020; Accepted: 26 August 2020; Published: date

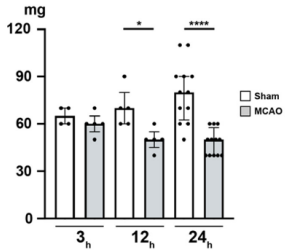

Figure S1. Temporal profile of the murine spleen weight after MCAO. The figure depicts the changes in splenic weight 3, 12, and 24 h after MCAO compared to sham-operated mice. The Mann–Whitney U-test was applied to calculate statistical differences. The data are presented as median ± IQR; $^{*}p < 0.05$, $^{****}p < 0.0001$.

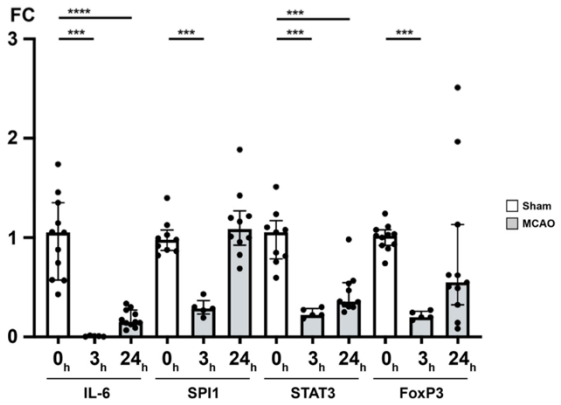

Figure S2. Temporal profile of immune cell egress from the murine spleen after MCAO. The figure shows the variations in the fold change (FC) of IL-6 and the transcription factors SPI1, STAT3, and FoxP3 in the murine spleen (3 and 24 h) after MCAO compared to sham. Fold change (FC) was normalized to the expression of GAPDH mRNA levels. The Mann–Whitney U-test was applied to calculate statistical differences. Data are presented as median ± IQR; $*p < 0.05$, $**p < 0.01$.

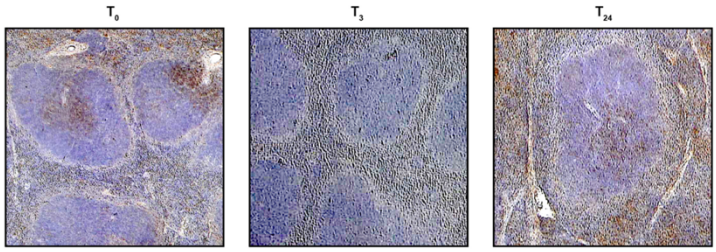

Figure S3. Splenic $CD3^+$ T cell egress. Temporal CD3 immunohistochemistry of sections from MCAO-operated mice. CD3 immunostaining is swiftly lost both from the white pulp, but equally, from the associated red pulp 3 h post-intervention (T_3). CD3 expression is regained in later stages after ischemia, suggesting a re-pooling of T cells back to the spleen.

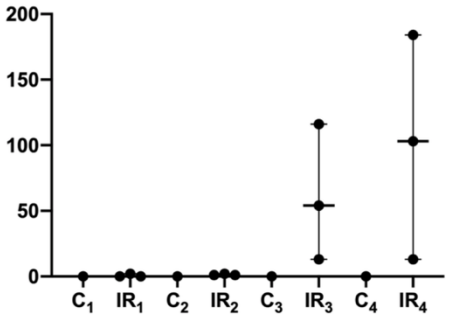

Figure S4. Quantification of CD3⁺ T cell recruitment to the brain. The figure details the number of infiltrated CD3⁺ T cells into the various cerebral areas denoted in Figure 4, i.e., region 1 (contralateral PIC), region 2 (contralateral peri-ventricular area (PVA)), region 3 (ipsilateral PVA), and region 4 (ipsilateral PIC). For each region, a comparison is made between sham-operated (C) and MCAO-operated mice (IR). Data are presented as median ± IQR; $n = 3$.

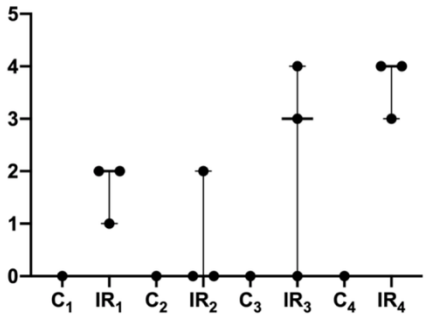

Figure S5. Quantification of FoxP3⁺ TREG cell recruitment to the brain. The figure details the number of infiltrated FoxP3⁺ T cells into the various cerebral areas denoted in Figure 5, i.e., region 1 (contralateral PIC), region 2 (contralateral peri-ventricular area (PVA)), region 3 (ipsilateral PVA), and region 4 (ipsilateral PIC). For each region, a comparison is made between sham-operated (C) and MCAO-operated mice (IR). Data are presented as median ± IQR; $n = 3$.